END

DATE
FILMED

10 .82

DTIC

AD A119258

ETL-0279

Inverse scattering applications
in determining terrain
feature parameters

Richard A. Hevenor

DECEMBER 1981
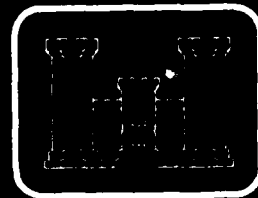
DTIC
ELECTE
SEP 1 5 1982
S    D
H

U.S. ARMY CORPS OF ENGINEERS
ENGINEER TOPOGRAPHIC LABORATORIES
FORT BELVOIR, VIRGINIA 22060

82 09 15 017

| REPORT DOCUMENTATION PAGE | | READ INSTRUCTIONS BEFORE COMPLETING FORM |
|---|---|---|
| 1. REPORT NUMBER ETL – 0279 | 2. GOVT ACCESSION NO. AD-A119 258 | 3. RECIPIENT'S CATALOG NUMBER |
| 4. TITLE (and Subtitle) INVERSE SCATTERING APPLICATIONS IN DETERMINING TERRAIN FEATURE PARAMETERS | | 5. TYPE OF REPORT & PERIOD COVERED Technical Report January 1980 – June 1980 |
| | | 6. PERFORMING ORG. REPORT NUMBER |
| 7. AUTHOR(s) Richard A. Hevenor | | 8. CONTRACT OR GRANT NUMBER(s) |
| 9. PERFORMING ORGANIZATION NAME AND ADDRESS U.S. Army Engineer Topographic Laboratories Fort Belvoir, Virginia 22060 | | 10. PROGRAM ELEMENT, PROJECT, TASK AREA & WORK UNIT NUMBERS 4A161101A91D |
| 11. CONTROLLING OFFICE NAME AND ADDRESS U.S. Army Engineer Topographic Laboratories Fort Belvoir, Virginia 22060 | | 12. REPORT DATE December 1981 |
| | | 13. NUMBER OF PAGES 45 |
| 14. MONITORING AGENCY NAME & ADDRESS(If different from Controlling Office) | | 15. SECURITY CLASS. (of this report) Unclassified |
| | | 15a. DECLASSIFICATION/DOWNGRADING SCHEDULE |

16. DISTRIBUTION STATEMENT (of this Report)

Approved for Public Release; Distribution Unlimited.

17. DISTRIBUTION STATEMENT (of the abstract entered in Block 20, if different from Report)

18. SUPPLEMENTARY NOTES

19. KEY WORDS (Continue on reverse side if necessary and identify by block number)

Inverse Scattering
Radar
Terrain Features
Vegetation

20. ABSTRACT (Continue on reverse side if necessary and identify by block number)
In this report, the results are described of an initial in-house research effort to investigate inverse scattering methods to determine terrain feature parameters. The problem of inverse scattering from discrete objects was considered, but was found not to apply to terrain feature extraction. Profile inversion concepts were analyzed, but were found to be only slightly relevant. Two specific inverse problems were analyzed and solved. The first problem involved solving for the dielectric constant of a slightly rough surface using the radar backscatter coefficients for two orthogonal polarizations. The second problem consisted of determining the dielectric constant and the conductivity of a medium located beneath a forest or jungle canopy. In this case, the electrical properties were calculated for two different polarizations of the incident wave.

## PREFACE

This study was conducted under ILIR Project 4A161101A91D, "Initial Research of Inverse Scattering Methods for Terrain Feature Analysis."

The study was done during the period January 1980 – June 1980 under the supervision of Dr. F. Rohde, Team Leader, Center for Theoretical and Applied Physical Sciences; and Mr. M. Crowell, Jr., Director, Research Institute.

COL Edward K. Wintz, CE was Commander and Director and Mr. Robert P. Macchia was Technical Director of the Engineer Topographic Laboratories during the report preparation.

Accession For

| NTIS GRA&I | ✓ |
| DTIC TAB | |
| Unannounced | |
| Justification | |

By

Distribution/

Availability Codes

| Dist | Avail and/or Special |

A

DTIC COPY INSPECTED

1

# CONTENTS

# ILLUSTRATIONS

# INVERSE SCATTERING APPLICATION
# IN DETERMINING TERRAIN
# FEATURE PARAMETERS

## INTRODUCTION

**Purpose.** The purpose of this research note is to present the results of a pre-liminary study of inverse scattering and its application in determining terrain feature parameters.

**Background.** The direct scattering problem consists of solving for a reflected or scattered wave, given a wave incident on a particular scatterer. In the solution to this problem, all the necessary physical, electrical, and statistical properties of the scatterer are assumed to be known, which then can be used to construct a model to calculate the scattered fields. Sometimes, however, various properties of a scatterer are not known. An example of this is the simulation of a layer of vegetation with a continuous random medium. To compute the scattered electric field from the random medium, one must know the two-point correlation function of the dielectric fluctuations. This correlation function has never been determined for vegetation of any type, and so the difficulty of calculating the scattered fields remains.

The inverse scattering problem is defined as using various properties of the scattered fields to compute certain physical or electrical properties of a scatterer. Several examples of inverse scattering problems will be considered briefly in this section. Later, in the analysis section, some of these examples will be developed in more detail.

One example of an inverse scattering problem is calculating the physical profile characteristics of a discrete object of revolution using the far field measurements of the radar cross section. In this problem, a discrete object of revolution is said to exist, and one makes radar scattering measurements as a function of incidence angle on the object. The radar scattering measurements are used to compute the radar cross section, which in turn is used to calculate the profile of the object via a particular set of inversion equations. Two basic techniques can be used to solve this problem, geometric optics and physical optics. The objects of interest are usually assumed to have infinite conductivity, which is a good assumption if one is trying to determine the profile characteristics of an aircraft, missile, or satellite.

4

Another example of an inverse problem is calculating the dielectric constant of a slightly rough surface using measurements of the radar backscatter coefficient for both horizontal and vertical polarizations, along with the first-order pertubation scattering models for a slightly rough surface. Because the dielectric constant of a soil can be related to moisture content, a solution to this inverse problem presents the possibility of determining quantitatively the soil moisture content in vast areas of desert type terrain.

Another example of an inverse problem is calculating the dielectric constant and conductivity of materials located beneath a forest canopy. A bistatic radar setup is used to measure amplitude and phase of the reflected field. The measurements are then used in the appropriate inversion equations to calculate the conductivity and dielectric constant of the medium below the canopy. These electrical properties can then be used to give a good indiçation of the nature of the material that is present. The derivation of these inversion equations, along with a complete analysis of this problem, will be presented later.

Another type of inversion problem involves solving a Fredholm linear integral equation of the first kind. Such integral equations arise in determining dielectric constant profiles as a function of soil depth or in computing the temperature profile of the atmosphere. The solution of these integral equations involves reducing the integral equation to a system of linear algebraic equations that must be solved by matrix inversion techniques. A great deal of research has been conducted on the solution of the Fredholm integral equation and its difficulties, such as stability and uniqueness.

In the analysis section, more detailed discussions will be presented of the inversion problems mentioned above. Computational results will be presented for the slightly rough surface problem and the forest canopy problem. In each of these two cases, the geometry of the problem to be solved will be presented, and the appropriate inversion equations will be derived. A discussion section will follow, in which side-looking airborne radar imagery will be considered for extracting terrain features. This is another example of an inversion problem as applied to terrain feature determinations.

# ANALYSIS

**Inverse Scattering for Discrete Objects.**    First, consider the scattering geometry of figure 1.
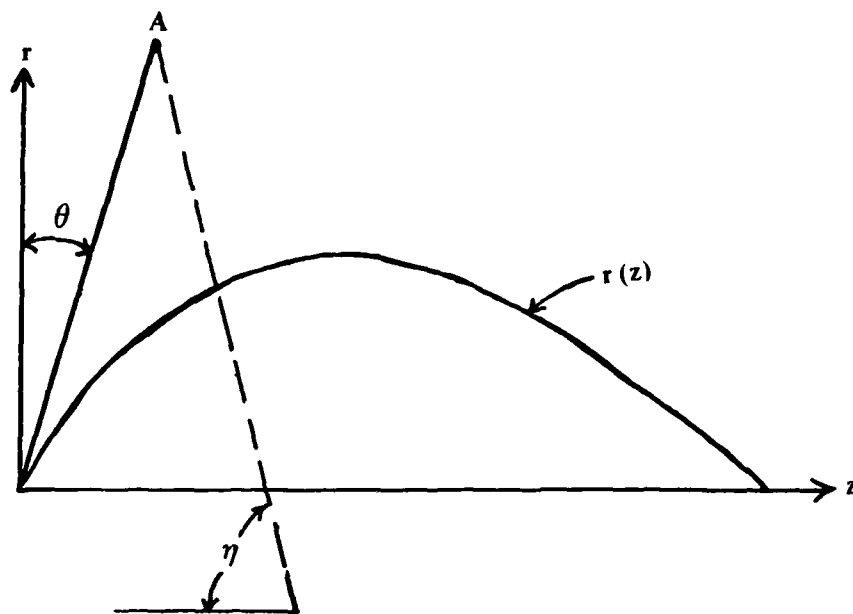


**FIGURE 1. Single Scatterers.**

An infinitely conducting object is formed by revolving the profile $r(z)$ about the $z$ axis. A radar at point A illuminates the object and measures the backscattered power in such a way that the radar cross section can be determined for the look direction $\eta$. The objective of this problem is to determine the object profile $r(z)$ from the remote sensing measurements of radar cross section as a function of $\eta$. Bojarski has derived a solution to this problem using a geometric optics approach that consists of the following two parametric equations:[1]

$$r^2(\eta) = \frac{2}{\pi} \int_0^{\eta} \sigma(\eta') \sin\eta' \cos\eta' \, d\eta' \tag{1}$$

$$z(\eta) = \frac{1}{\pi} \int_0^{\eta} \frac{\sigma(\eta')}{r(\eta')} \sin^2\eta' \, d\eta' \tag{2}$$

where $\sigma(\eta)$ is the radar cross section as a function of look direction. The advantage of using the above equations is that no phase information is required to obtain the profile $r(z)$. The disadvantage is that the radar cross section must be known for all values of $\eta$ from 0 to $\pi$. In addition, there are restrictions on the curvature of $r(z)$ in order for the above equations to hold.

Bojarski has also derived expressions to determine $r(z)$ for an object using a physical optics approach.[2] The starting point for this derivation is the equation for the scattered magnetic field given below:

$$\underline{H}_s = \frac{1}{4\pi} \oint_S (\underline{n} \times \underline{H}) \times \nabla\phi \, ds \tag{3}$$

---

[1] Norbert N. Bojarski, *Signal Processing Studies and Analysis--A Study of Electromagnetic Inverse Scattering*, Syracuse University Research Corporation, Technical Report No. RADC-TR-66-830, April 1967, AD 813 981.

[2] Ibid.

7

where

> $\underline{H}_s$ is the scattered magnetic field from the object.
>
> $\underline{n}$ is a unit vector normal to the surface of the object.
>
> $\underline{H}$ is the total magnetic field at the surface of the object.
>
> $\phi$ is the free space scalar Green's function.

Making the infinite conductivity assumption for the object, Bojarski derives the following result for $r(z)$:[3]

$$r(z) \;=\; \frac{1}{2k_o} \, \arg \left\{ \sqrt{j} \int_{-\pi/4}^{\pi/4} e^{2jk_o z \sin\theta} \; \rho(\theta) \cos^{1/2}\theta \, d\theta \right\} \tag{4}$$

where

$$j = \sqrt{-1}$$

> $k_o$ is the free space propagation constant equal to $2\pi/\lambda$, where $\lambda$ is the wavelength
>
> $\rho(\theta)$ is related to the radar cross section as follows:

$$\sigma = \rho \, \rho^* \tag{5}$$

---

[3]Norbert N. Bojarski, *Signal Processing Studies and Analysis--A Study of Electromagnetic Inverse Scattering,* Syracuse University Research Corporation, Technical Report No. RADC-TR-66-830, April 1967, AD 813 981.

Since $\rho$ is complex, the amplitude and phase of the received signal must be measured. The parameter $\rho$ is called the complex scalar field cross section and can be related to the scattered electric field as follows:

$$\rho = 2\sqrt{\pi}\, R\, \frac{E_s}{E_i} \tag{6}$$

where

R   is the far field distance from the object to the radar.

$E_s$ is the scattered electric field.

$E_i$ is the electric field incident on the object.

The three equations (1), (2), and (4) provide two methods for detern   g the profile function $r(z)$ of an infinitely conducting object of revolution.

These kinds of inverse scattering problems appear to not apply to the problem of terrain feature extraction, because terrain consists of many scattering objects of complicated geometry and finite conductivity.

**Profile Inversion.**   Many inverse problems in remote sensing can be formulated in terms of a Fredholm integral equation of the first kind as given below:

$$g(y) = \int_a^b K(y, x)\, f(x)\, dx \tag{7}$$

9

In the above equation, $K(y, x)$ forms the kernel of the integral. Measurements are made at various values of $y$ to give $g$. The objective of these problems is to determine $f(x)$ from a knowledge of $K(y, x)$ and a finite set of measurements of $g(y)$. Twomey has written about techniques for the solution of the above integral equation.[4] Even if we assume perfect precision in making the measurements of $g(y)$, the questions of existence and uniqueness still exist. Equation (7) represents a mathematical model of some physical process and, as such, contains simplifications and approximations that may or may not be valid at the time the measurements for $g(y)$ are made. If the approximations are not valid, the existence of any useful solution is extremely doubtful, even if the measurements contain no errors. If the model is shown to be valid, then one must address the question of uniqueness. Given a set of measurements for $g(y)$, a solution for $f(x)$ can be determined, but the question is whether or not the solution is unique. Other solutions may exist that are just as valid and physically realizable. Many times, experimental measurements contain errors of various kinds, and for certain problems employing equation 7, this leads to *ill-posed* problems. An *ill-posed* problem is defined as one in which small measurement errors in $g(y)$ lead to large fluctuations in $f(x)$. Although the difficulties associated with existence, uniqueness, and *ill-posed* problems have been investigated many times, they are still the subjects of much research.

**Example of a Real Profile Inversion Problem.** In determining earth conductivity with depth surface current measurements are made using two parallel conductors lying on the surface of the ground with a separation distance $x$ and a potential difference $v$ applied between them. The resulting electric field distribution $E(x, z)$ is a function of the separation distance $x$ and the depth $z$ in the soil. This electric field distribution can be computed if the permittivity of the soil is constant or varies in a known way. The conductivity of the soil $\sigma(z)$ varies with depth and can be related to the current $i(x)$ in the conductors as follows:

$$i(x) = \int^{\infty} E(x, z) \sigma(z) \, dz \tag{8}$$

[4]S. Twomey, *Introduction to The Mathematics of Inversion in Remote Sensing and Indirect Measurements*, Elsevier Scientific Publishing Company, 1977.

By making measurements of the current and the electric field distribution for various values of x, one can determine the conductivity profile if the integral equation can be inverted.

To obtain a numerical solution to an integral equation like the Fredholm equation, one must rely on the approximation of the integral by a sum, that is, an appropriate numerical integration formula, such as Simpson's Rule, must be chosen and the integral equation given in (7) reduced to a matrix equation of the following form:

$$\underline{g} = \underline{A} \times \underline{f} \tag{9}$$

where $\underline{g}$ is an $M \times 1$ matrix corresponding to the $M$ measurements that have been made. The objective is now to solve the matrix equation in (9) for the appropriate values of $\underline{f}$.

**Calculating of the Dielectric Constant for a Slightly Rough Surface.** Now consider an elementary example of an inverse scattering problem in which a solution for the dielectric constant of a slightly rough surface is obtained in terms of the horizontally and vertically polarized radar backscatter coefficients. The scattering geometry of the problem to be solved is shown in figure 2.

A plane wave with a harmonic time dependence of $\exp(j\omega t)$ is incident onto the slightly rough dielectric surface $s(x, y)$ at an angle of incidence $\theta_i$. The medium above the surface $s(x, y)$ is assumed to be free space and has the propagation constant $k_o$. The propagation constant in the medium below the surface is $k$. The equations for the radar backscatter coefficient for horizontal and vertical polarizations are given as

$$\sigma^o_{hh}(\theta_i) = 8\sigma_1^2 k_o^4 \cos^4\theta_i \, R_\perp^2 \, W(2k_o \sin\theta_i, 0) \tag{10}$$

$$\sigma^o_{vv}(\theta_i) = \tag{11}$$

$$\frac{2\sigma_1^2 k_o^2 \cos^2\theta_i (k_o^2 - k^2)^2 \, [k\cos\phi(1 - R_{\parallel}) \cos\theta_i + k_o \sin^2\theta_i(1 + R_{\parallel})]^2 \, W(2k_o \sin\theta_i, 0)}{k^2 \, (k \cos\theta_i + k_o \cos\phi)^2}$$
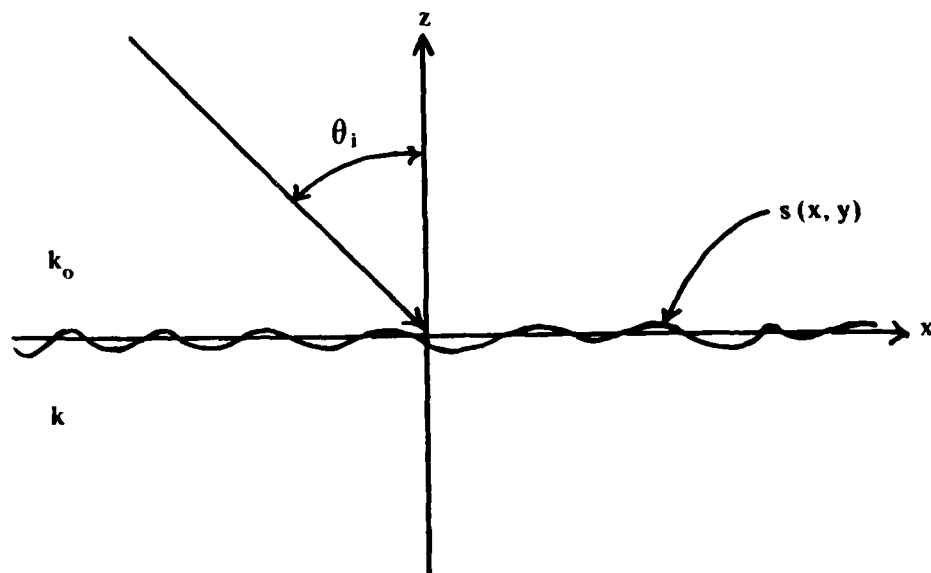
11

**FIGURE 2. Slightly Rough Surface.**

where

$\sigma^{\circ}_{hh}(\theta_i)$ is the radar backscatter coefficient for the case of horizontal polarization transmit and horizontal polarization receive, $\sigma^{\circ}_{vv}(\theta_i)$ is the radar backscatter coefficient for the case of vertical polarization transmit and vertical polarization receive,

$\sigma_l$ is the standard deviation of the rough surface undulations of $s(x, y)$

$$k \cos \phi = \sqrt{k^2 - k_o^2 \sin^2 \theta_i}$$

$W(2k_o \sin\theta_i, 0)$ is the surface roughness spectrum and is equal to the two-dimensional Fourier transform of the autocorrelation function of $s(x, y)$, and $R_{\perp}$ and $R_{\parallel}$ are the Fresnel reflection coefficients for horizontal and vertical polarizations, respectively, and are given as

12

$$R_\perp = \frac{k_o \cos\theta_i - \sqrt{k^2 - k_o^2 \sin^2\theta_i}}{k_o \cos\theta_i + \sqrt{k^2 - k_o^2 \sin^2\theta_i}} \qquad (12)$$

$$R_\| = \frac{k^2 \cos\theta_i - k_o \sqrt{k^2 - k_o^2 \sin^2\theta_i}}{k^2 \cos\theta_i + k_o \sqrt{k^2 - k_o^2 \sin^2\theta_i}} \qquad (13)$$

$k = \omega \sqrt{\mu_o \epsilon_o \epsilon_r}$ where $\epsilon_r$ is the relative dielectric constant of the medium below the rough surface $s(x, y)$.

Equations (10) and (11) are derived from the first-order perturbation theory, which uses a two-dimensional Fourier transform representation for the scattered fields. The basic requirement that equations (10) and (11) must obey is that $k_0 \sigma_l$ must be less than one. This is because a perturbation approach is used for the solution, and only first-order terms are considered. In equations (10) and (11), the back-scatter coefficients are not only functions of the dielectric constant $(\epsilon_r)$ and incidence angle $(\theta_i)$ but also functions of the surface roughness parameters. Any attempt to determine the dielectric constant from either (10) or (11) will require a knowledge of the backscatter coefficient and of the surface roughness properties. A solution should be obtained for the dielectric constant $(\epsilon_r)$ in terms of remote sensing measurements such as the backscatter coefficient. The dielectric constant can be directly related to moisture content, and if a solution for the dielectric constant can be found in terms of backscatter coefficient, a quantitative way of determining soil moisture will have been found.

However, it cannot be assumed that knowledge of the rough surface properties exists for a typical terrain surface for which equations (10) and (11) are valid. On the other hand, if equation (10) is divided by equation (11), the rough surface properties cancel out and are no longer required.

Let

$$f_{hv}(\theta_i) = \sigma^\circ_{hh}(\theta_i) \Big/ \sigma^\circ_{vv}(\theta_i) \qquad (14)$$

13

then

$$f_{hv}(\theta_i) = \frac{4k_o^2 \cos^2\theta_i \, R_\perp^2 k^2 \, (k\cos\theta_i + k_o\cos\phi)^2}{(k_o^2 - k^2)^2 [k\cos\phi \, (1 - R_{\parallel})\cos\theta_i + k_o\sin^2\theta_i \, (1 + R_{\parallel})]^2}$$

(15)

In figure 3, the results are presented for computing $f_{hv}(\theta_i)$ for two values of $\epsilon_r$ over an angular range of 0 to 80 degrees. We see that when $\theta_i = 0°$, $f_{hv}(\theta_i)$ is equal to one for both dielectrics. This is because when $\theta_i$ is equal to $0°$, the horizontal and vertical polarizations will give the same result. As the angle of incidence is increased, the larger value of $\epsilon_r$ makes $f_{hv}(\theta_i)$ fall off faster. Taking the square root of (15) leads to the following result:

$$f(k) = (k_o^2 - k^2)\sqrt{f_{hv}(\theta_i)} \, [k\cos\phi(1 - R_{\parallel})\cos\theta_i + k_o^2\sin^2\theta_i(1 + R_{\parallel})]$$

$$- 2k_o R_\perp \cos\theta_i \, (k^2\cos\theta_i + k_o k\cos\phi) = 0$$

(16)

Equation (16) can be used to obtain a solution for $k$ and, hence, $\epsilon_r$ by employing the Newton-Raphson numerical methods technique. In this method, the $n + 1^{st}$ estimate of $k$ is related to the $n^{th}$ estimate as follows:

$$k_{n+1} = k_n - \frac{f(k_n)}{f'(k_n)}$$

(17)

The prime on $f'$ is used to indicate a derivative of $f$ with respect to $k$. An expression for this derivative can be written as follows:

$$f'(k) = \frac{df}{dk} = -2k\sqrt{f_{hv}(\theta_i)} \, [k\cos\phi \, (1 - R_{\parallel}) \cos\theta_i + k_o\sin^2\theta_i \, (1 + R_{\parallel})]$$

$$+ \sqrt{f_{hv}(\theta_i)}(k_o^2 - k^2) \left[ \frac{d(k\cos\phi)}{dk} (1 - R_{\parallel})\cos\theta_i + \frac{dR_{\parallel}}{dk}(k_o\sin^2\theta_i \right.$$
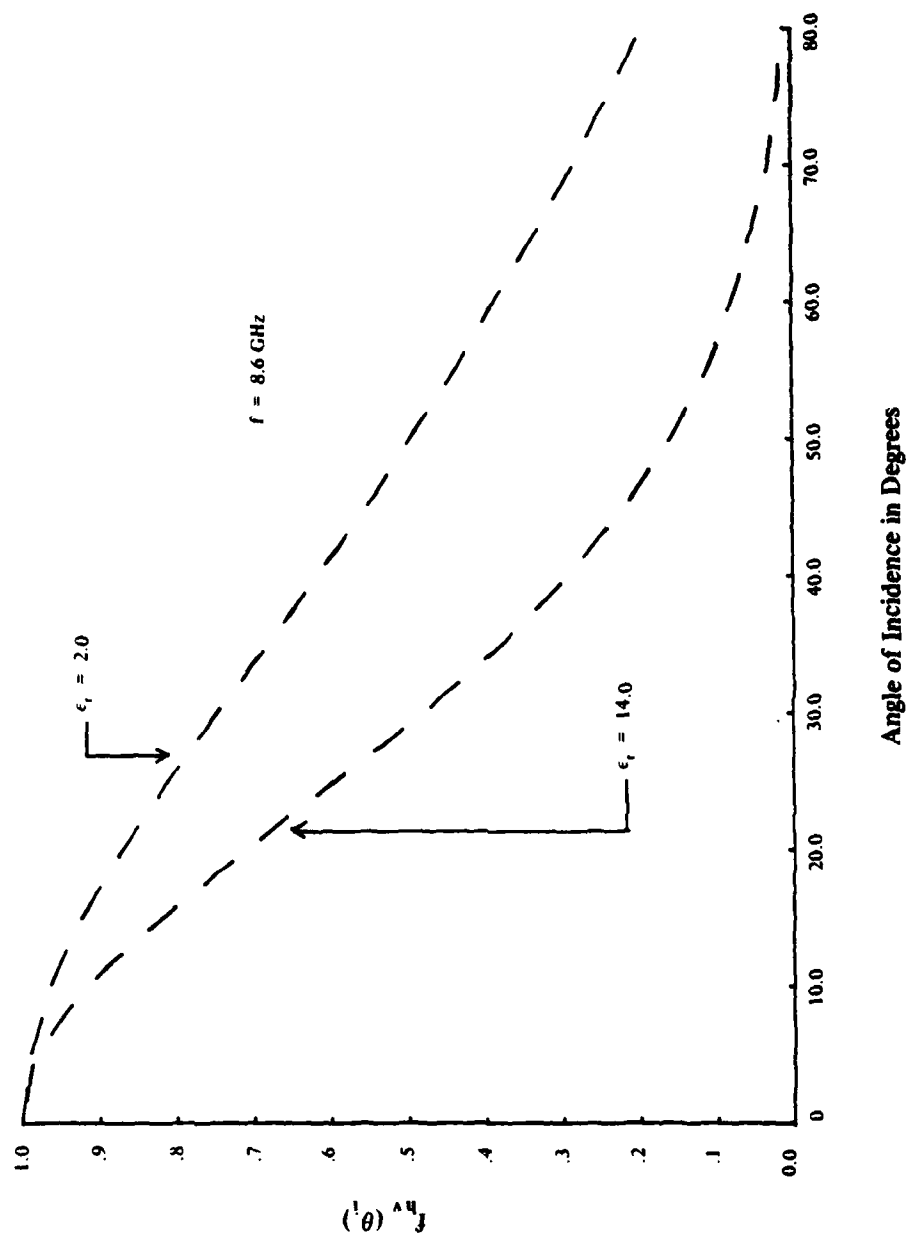
14

FIGURE 3. Study of $f_{hv}(\theta_i)$ Variations With $\epsilon_r$.

15

$$\left. - k\cos\phi \, \cos\theta_i\right] - 2k_o\cos\theta_i \left[ \frac{dR_\perp}{dk}(k^2\cos\theta_i + k_o\, k \cos\phi)\right.$$

$$\left. + R_\perp \, (2k\cos\theta_i + k_o\,\frac{d(k\cos\phi)}{dk})\right] \tag{18}$$

To compute $f'(k)$, there is a need to calculate $\dfrac{dR_\perp}{dk}$, $\dfrac{dR_\parallel}{dk}$ and $\dfrac{d(k\cos\phi)}{dk}$. These three derivatives can be computed from the equations given previously.

$$\frac{dR_\perp}{dk} = \frac{-2k\,k_o\cos\theta_i}{(k^2 - k_o^2\sin^2\theta_i)^{\frac{1}{2}} \,\{k_o\cos\theta_i + \sqrt{k^2 - k_o^2\sin^2\theta_i}\}^2} \tag{19}$$

$$\frac{dR_\parallel}{dk} = \frac{2k_o\, k\cos\theta_i \,[2\widetilde{W}^2 - k^2]}{\widetilde{W}\,[k^2\cos\theta_i + k_o\,\widetilde{W}]^2} \tag{20}$$

where

$$\widetilde{W} = \sqrt{k^2 - k_o^2\sin^2\theta_i}$$

$$\frac{d(k\cos\phi)}{dk} = \frac{k}{\sqrt{k^2 - k_o^2\sin^2\theta_i}} = k/\widetilde{W} \tag{21}$$

To validate using (17) to compute $k$ and $\epsilon_r$, a computer program was written to solve the direct scattering problem from equations (10) and (11). Particular values were chosen for $\sigma_1$, $\theta_i$, and $\epsilon_r$. A form for the roughness spectrum $W(2k_o\sin\theta_i,0)$ was assumed and values were calculated for $\sigma_{hh}^o$ and $\sigma_{vv}^o$. These values were then used to compute $f_{hv}(\theta_i)$ from (14). This value of $f_{hv}(\theta_i)$ was used to calculate $k$ from (17). It was found that for values of $\theta_i$ greater than zero, $\epsilon_r$ could be determined from (17). Thus, the inversion technique and equations were verified. If further work on this problem is warranted, experimental measurements should be conducted, perhaps in a desert area to determine $\sigma_{hh}^o$ and $\sigma_{vv}^o$ as a function of incidence angle. Also, ground truth data would have to be collected, such as dielectric constant and soil moisture content. This approach would enable the inversion techniques to be analyzed using experimental data.

16

**Calculating the Dielectric Constant and Conductivity for a Medium Beneath a Forest or Jungle Canopy — Horizontal Polarization.** Let's now consider an inverse problem in which a solution is sought for the dielectric constant and the conductivity of a medium beneath a forest or jungle canopy. The geometry for this problem is presented in figure 4.

The simplest electromagnetic model for a forest canopy consists of a lossy dielectric slab over a flat earth. The forest is of height $d$ and is considered to have an average dielectric constant $(\epsilon_2)$ and an average conductivity $(\sigma_2)$. This simple model for a forest or jungle is a good approximation for frequencies less than 200 MHz. Although even in this frequency range, one must often incorporate anisotropic effects. The propagation of electromagnetic waves in forested media has been studied extensively for frequencies less than 200 MHz. (see Wait, et al.)[5] These studies were conducted to further the effort of point-to-point communications in a forest environment. Our problem, however, is to invert the remote sensing equations to obtain a solution for the electrical properties of the ground $(\epsilon_1, \sigma_1)$ in terms of the far field reflectivity. One of the difficulties in dealing with problems of forested media is how to determine the average electrical parameters $\epsilon_2$, and $\sigma_2$. Hagn discusses various techniques that can be used to determine the electrical properties of forests and presents some results for two different jungle sites in Thailand.[6] In figure 4, a bistatic radar setup is indicated in medium 3 to measure the reflected electric field. Below the forest, the ground surface is assumed to be flat with a dielectric constant $\epsilon_1$ and a conductivity $\sigma_1$. A horizontally polarized plane wave with a harmonic time dependence of $\exp(j\omega t)$ is incident onto the forest medium at an angle of incidence $\theta_i$. The total electric field in medium three $(E_3(r))$ can be written as follows:

$$E_3(r) = \underline{a}_y E_o \left\{ e^{-jk_o z \cos\theta_i} + R_\perp e^{jk_o z \cos\theta_i} \right\} e^{-jk_o x \sin\theta_i} \tag{22}$$

[5] J. R. Wait, R. H. Ott, and T. Telfer, (Editors), "Work Shop on Radio System in Forested and or Vegetated Environments," Technical Report No. ACC–ACO–1–74, Institute for Telecommunication Sciences, U. S. Department of Commerce, Boulder, Colorado.

[6] Hagn, G.H., *Electrical Properties of Forested Media* in the "Work Shop on Radio System in Forested and or Vegetated Environments," Technical Report No. ACC–ACO–1–74, Institute for Telecommunication Sciences, U.S. Department of Commerce, Boulder, Colorado.
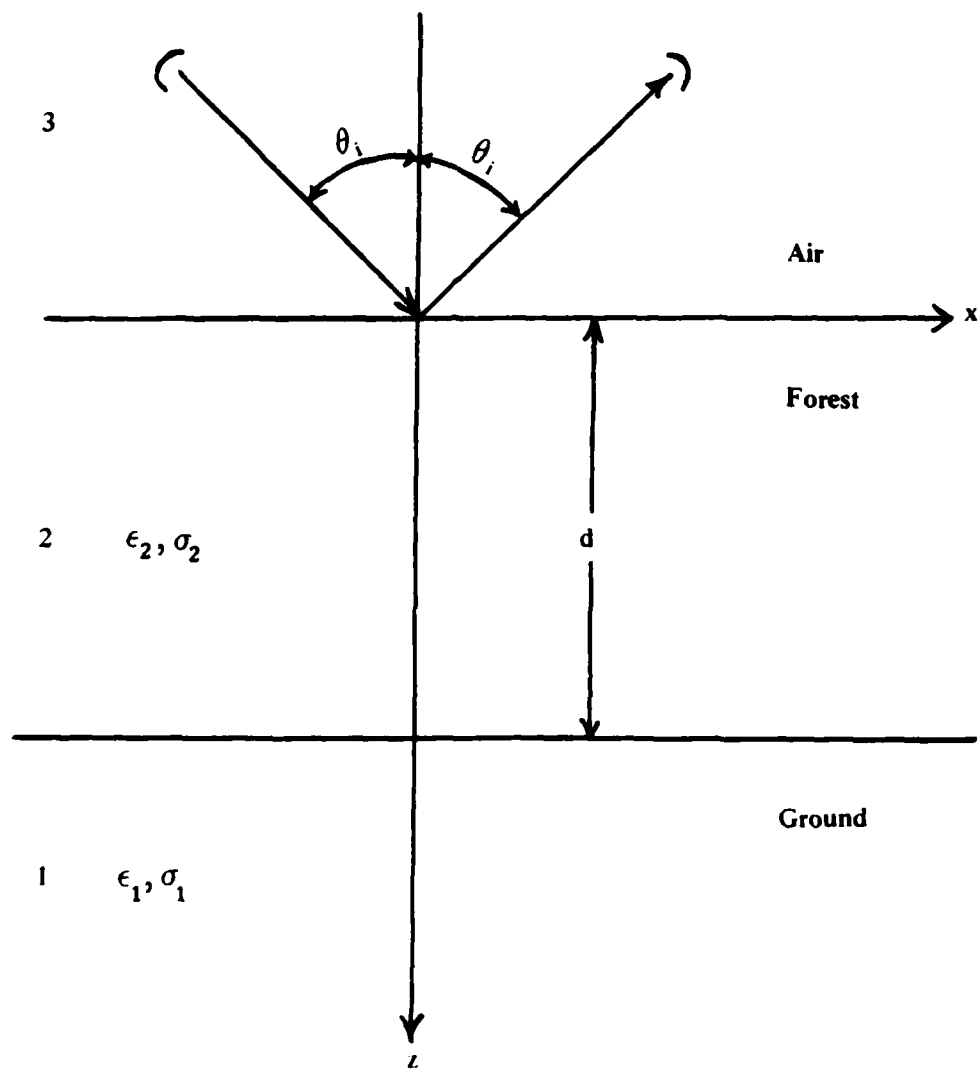
FIGURE 4. Reflection From a Forest Canopy.

18

where

$\underline{a}_y$ is a unit vector in the $y$ direction.

$E_o$ is the amplitude of the incident electric field.

$R_\perp$ is the reflection coefficient.

The first term on the right side of (22) represents the incident field. The second term represents the reflected field. The reflection coefficient can be written in terms of the impedances of the three media involved.

$$R_\perp = \frac{Z_{inh}^{(2)} - Z_{3h}}{Z_{inh}^{(2)} + Z_{3h}} \tag{23}$$

where

$$Z_{inh}^{(2)} = \frac{Z_{2h}(Z_{1h} + Z_{2h}) + Z_{2h}(Z_{1h} - Z_{2h})e^{-j2k_2 d \cos\theta_2}}{Z_{1h} + Z_{2h} - (Z_{1h} - Z_{2h})e^{-j2k_2 d \cos\theta_2}} \tag{24}$$

$$Z_{3h} = \frac{\omega\mu_o}{k_o \cos\theta_i} \qquad Z_{2h} = \frac{\omega\mu_o}{k_2 \cos\theta_2} \qquad Z_{1h} = \frac{\omega\mu_o}{k_1 \cos\theta_1}$$

$$k_o \sin\theta_i = k_1 \sin\theta_1 = k_2 \cos\theta_2$$

The parameters $k_0$, $k_2$, and $k_1$ represent the propagation constants in air, in the forest layer, and in the ground, respectively. Although $k_2$ and $k_1$ are both complex, $k_0$ will be real. Because we are dealing with complex propagation constants, the reflection coefficient will also be complex and can be written as

$$R_\perp = \rho_\perp e^{j\phi_\perp} \tag{25}$$

19

where $\rho_1$ represents the magnitude of $R_1$ and $\phi_1$ is the phase. In figures 5 through 8, curves are presented of $\rho_1$ versus incidence angle for three different materials below the forest canopy. The three materials are loam soil, water, and aluminum. The electrical properties of these materials are given below:

| | $\epsilon_{r1} = \epsilon_1 / \epsilon_0$ | $\sigma_1$ (mhos / meter) |
|---|---|---|
| Loam Soil 13.77% Water | 14.5 | 0.0105 |
| Water | 80 | 0.000234 |
| Aluminum | 1.0 | $3.53 \times 10^7$ |

The values used for $\epsilon_2$ and $\sigma_2$ are $1.01\epsilon_0$ and $4 \times 10^{-5}$ mho/meter, respectively. These numbers were taken from Hagn and represent the parameters for a jungle site in Thailand.[7] The height of the forest was assumed to be 20 meters. Figure 5 presents curves for a frequency of 30 MHz. The oscillations that occur in the curves are due to the influence of the forest layer. At large angles of incidence, the three curves tend to merge, indicating that the three materials would be indistinguishable from one another. As the frequency decreases, notice that the forest layer has less and less influence on $\rho_1$, until finally in figure 8, at 3 MHz, all three curves are completely monotonic. Also, in figure 8, the water and the loam soil would be indistinguishable for all angles of incidence. In figure 9 and 10, curves are shown of $\phi_1$ in degrees versus angle of incidence for the loam soil and water. In figure 11, curves are shown of $\rho_1$ versus frequency for the three materials at an angle of incidence of $30^\circ$. In attempting to obtain a solution for $\epsilon_1$ and $\sigma_1$, assume that both the amplitude and phase of the reflected field are measured. This would then enable a complete determination to be made of $R_1$. Using this knowledge of $R_1$, we will seek to invert equations (23) and (24) and obtain a solution for $\epsilon_1$ and $\sigma_1$ in terms of $R_1$, d, $\epsilon_2$, $\sigma_2$, $\theta_i$ and frequency. By combining equations (23) and (24), one obtains:

[7]Hagn, G.H., *Electrical Properties of Forested Media* in the "Work Shop on Radio System in Forested and or Vegetated Environments," Technical Report No. ACC-ACO-1-74, Institute for Telecommunication Sciences, U.S. Department of Commerce, Boulder, Colorado.
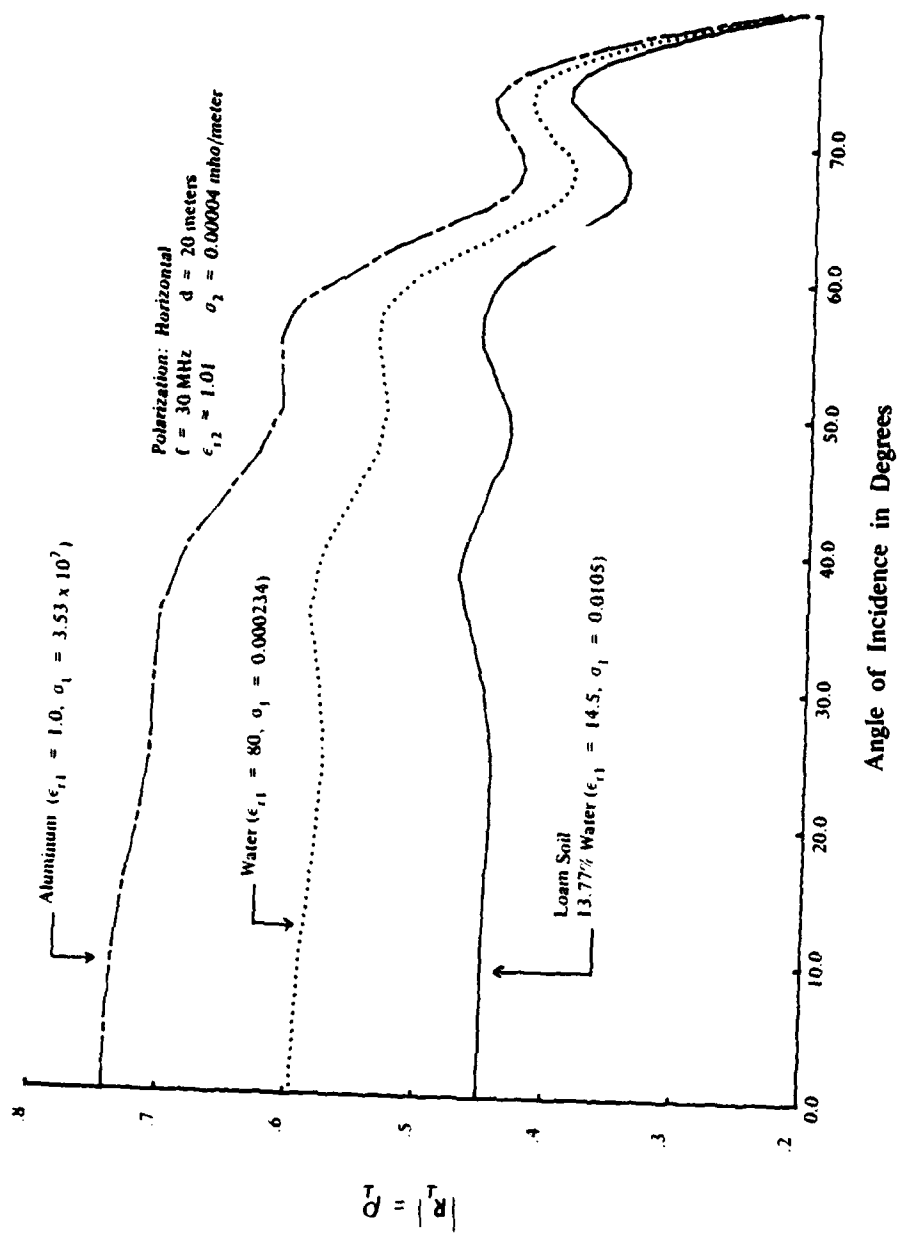
20

**FIGURE 5. Study of Reflection Coefficient Versus Angle of Incidence -- Horizontal Polarization.**
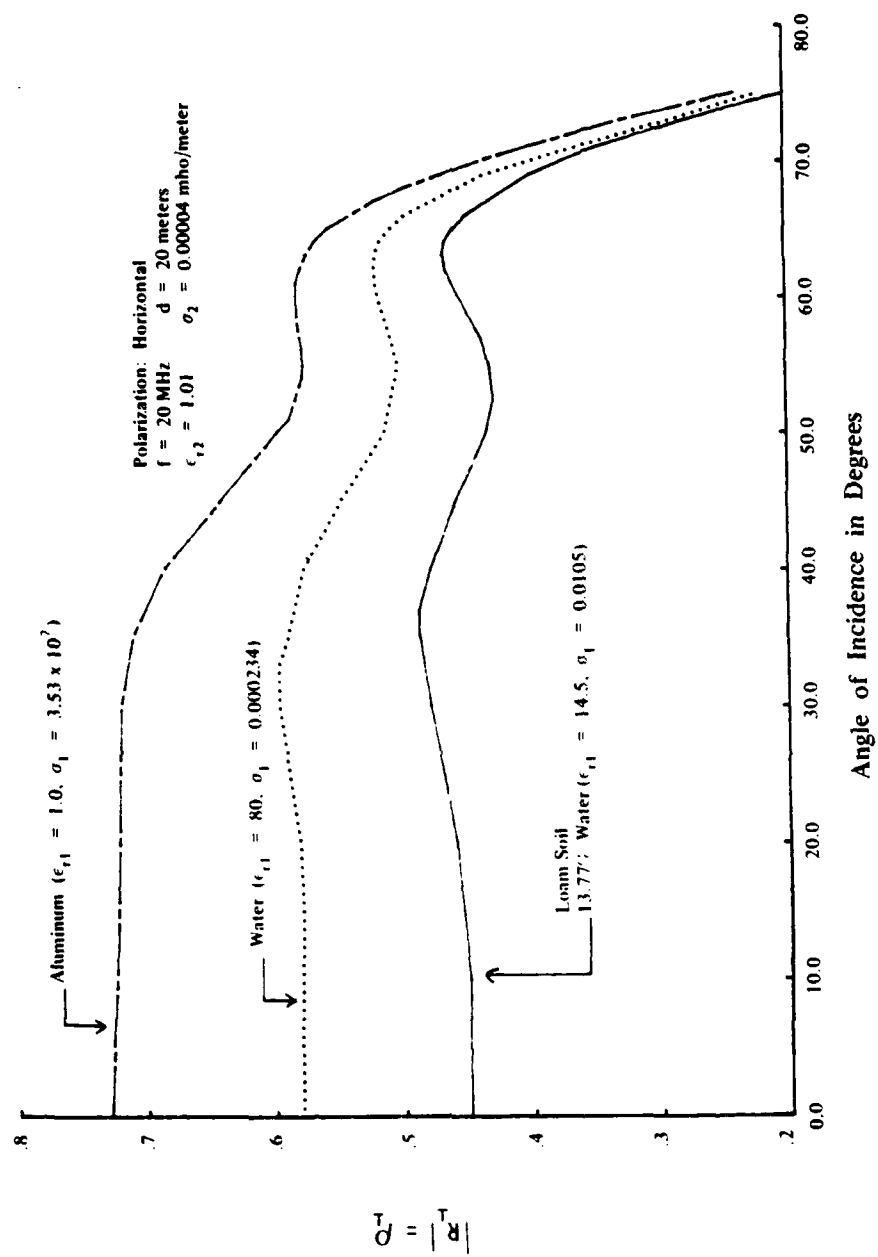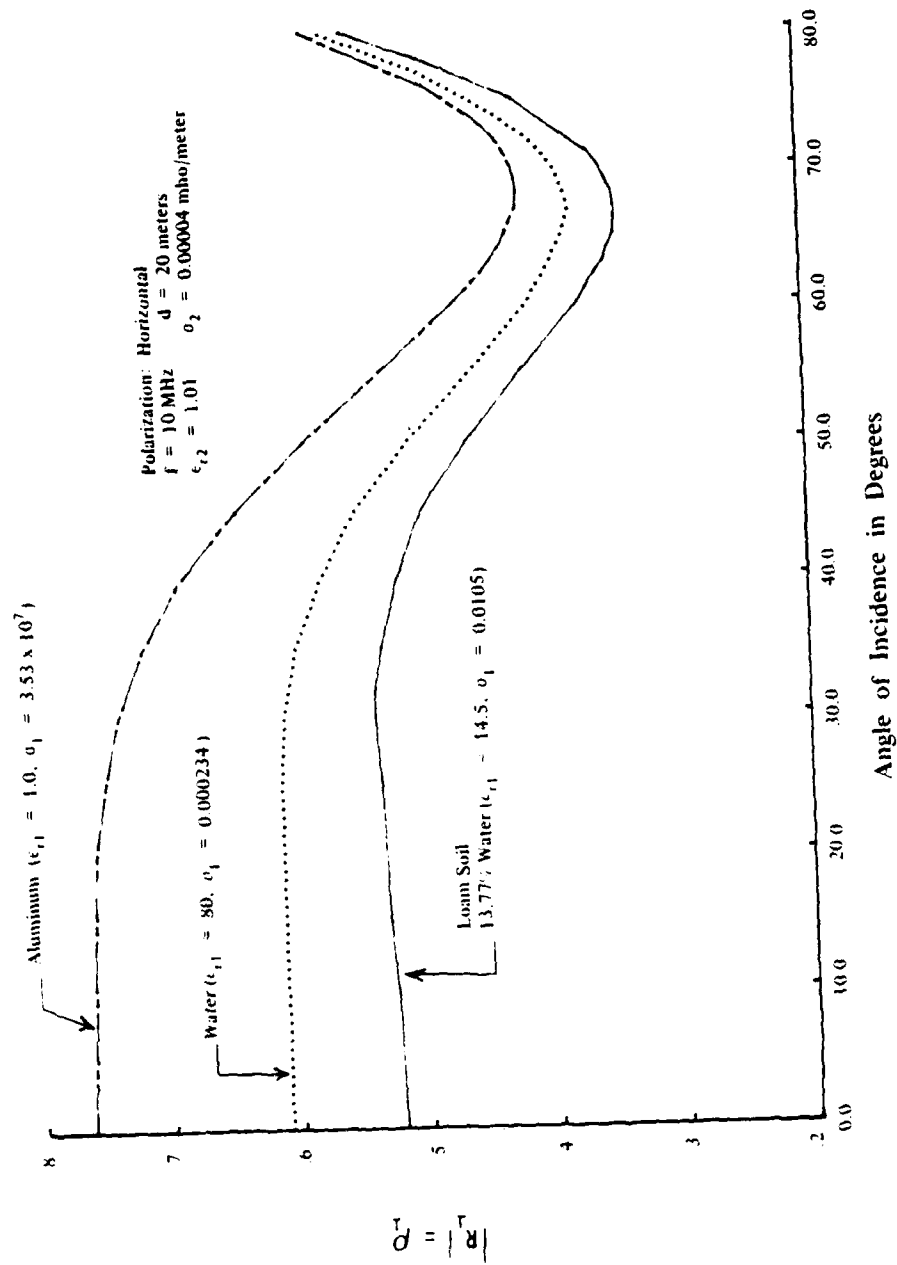
21

FIGURE 6. Study of Reflection Coefficient Versus Angle of Incidence -- Horizontal Polarization.

22

FIGURE 7. Study of Reflection Coefficient Versus Angle of Incidence -- Horizontal Polarization.

Polarization: Horizontal
$f = 10$ MHz $\quad$ d $= 20$ meters
$\epsilon_{r2} = 1.01$ $\quad$ $\sigma_2 = 0.00004$ mho/meter

Aluminum ($\epsilon_{r1} = 1.0$, $\sigma_1 = 3.53 \times 10^7$)

Water ($\epsilon_{r1} = 80$, $\sigma_1 = 0.000234$)

Loam Soil
13.77% Water ($\epsilon_{r1} = 14.5$, $\sigma_1 = 0.0105$)

Angle of Incidence in Degrees
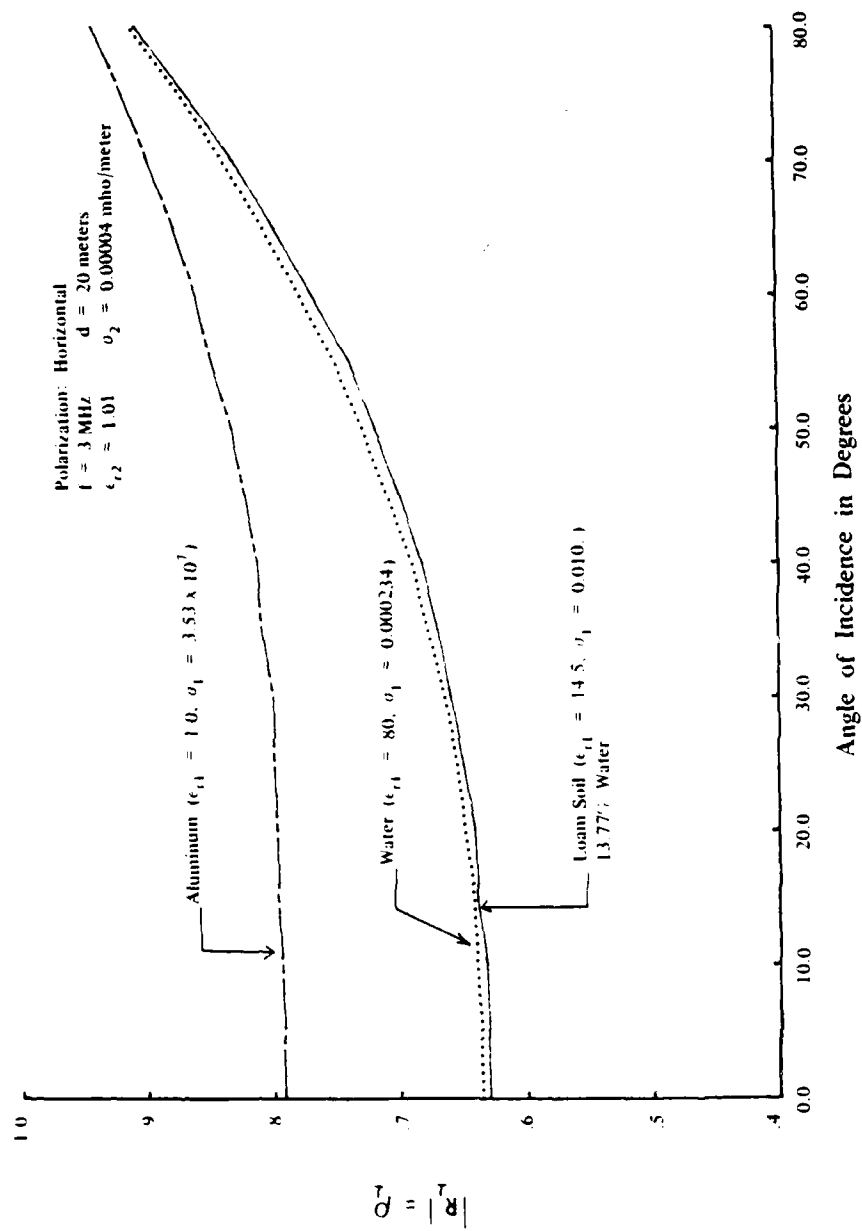
$|R_\perp| = \rho_\perp$

23

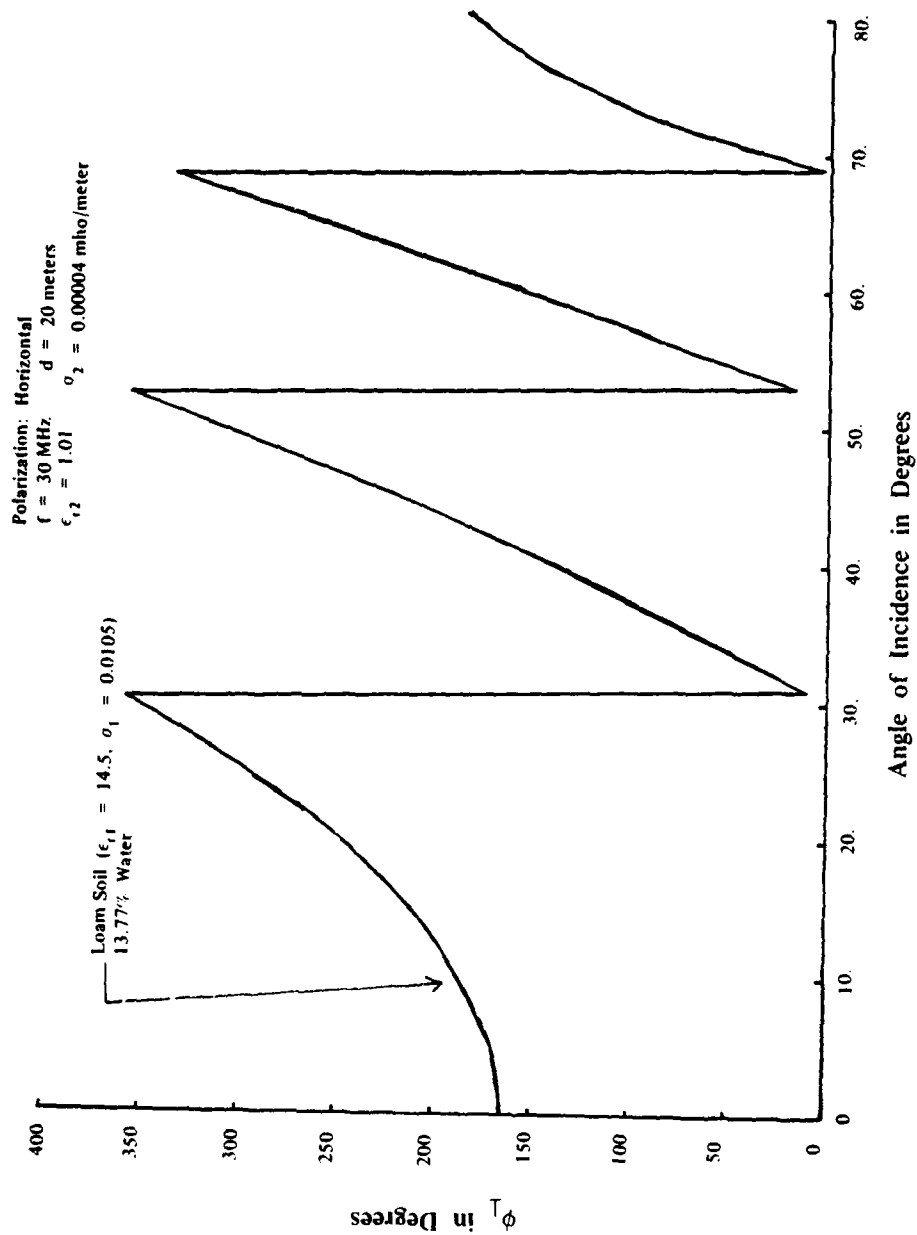FIGURE 8. Study of Reflection Coefficient Versus Angle of Incidence -- Horizontal Polarization.

24

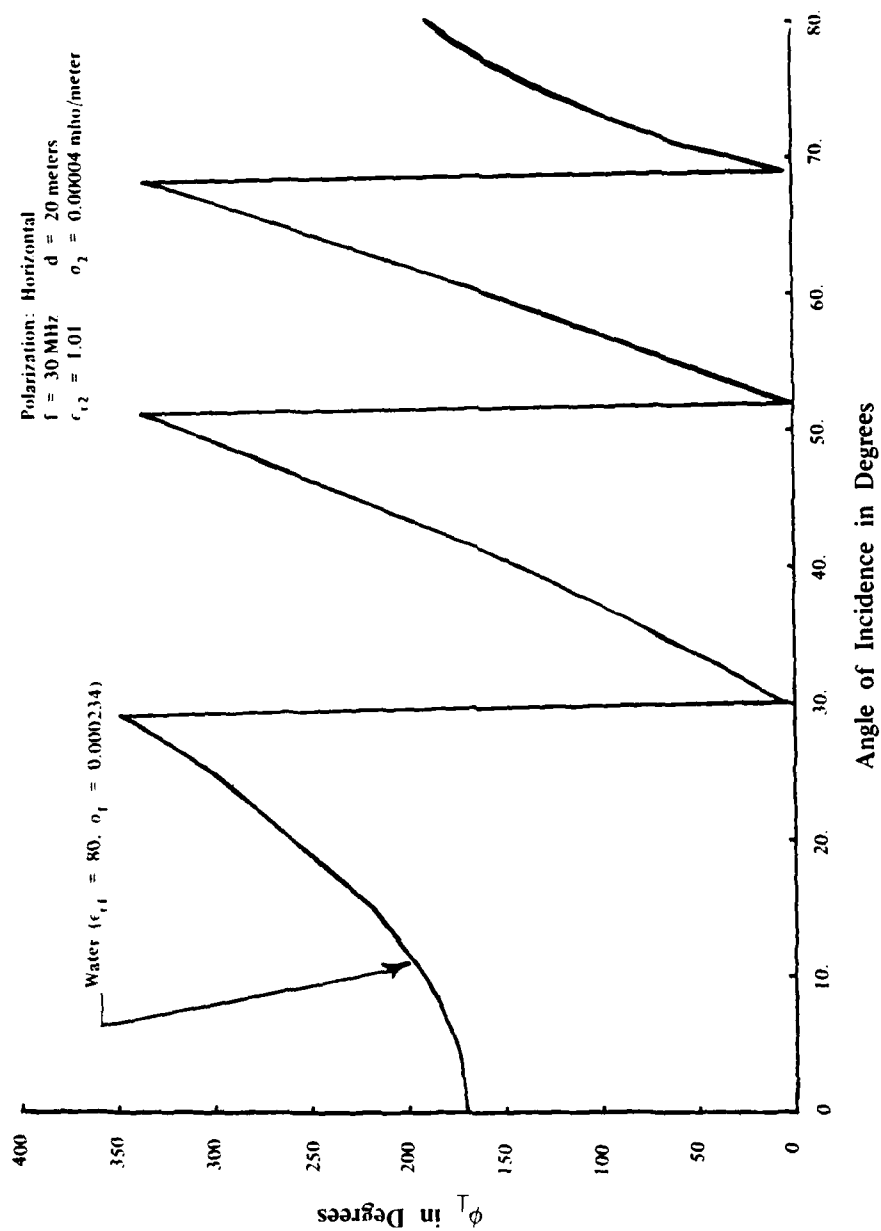FIGURE 9. Study of Phase Versus Angle of Incidence for Loam Soil -- Horizontal Polarization.

25

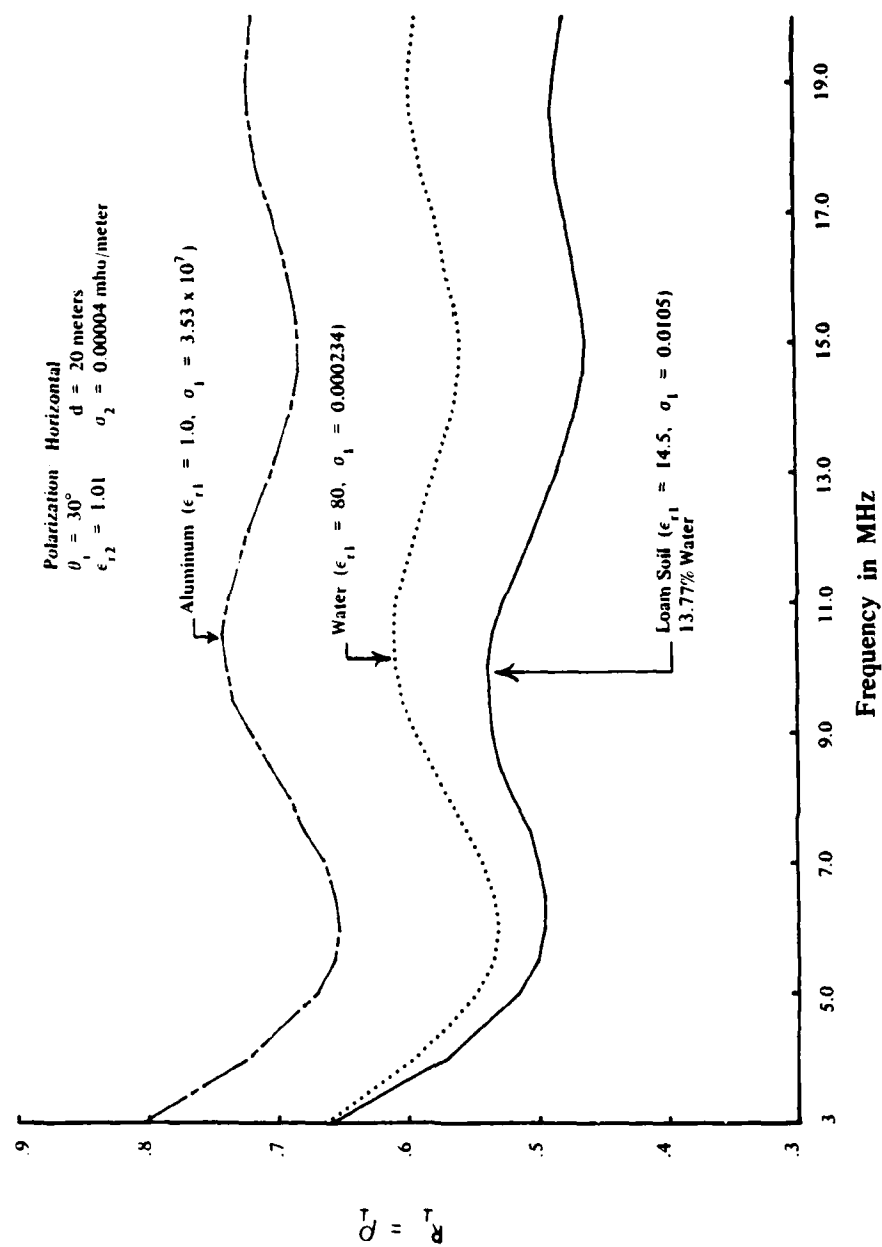FIGURE 10. Study of Phase Versus Angle of Incidence for Water -- Horizontal Polarization.

26

FIGURE 11. Study of Reflection Coefficient Versus Frequency – Horizontal Polarization.

27

$$Z_{inh}^{(2)} = \frac{Z_{3h}(1 + R_\perp)}{1 - R_\perp} = \frac{Z_{2h}(Z_{1h} + Z_{2h}) + Z_{2h}(Z_{1h} - Z_{2h})\exp(-2jk_2 d \cos\theta_2)}{Z_{1h} + Z_{2h} - (Z_{1h} - Z_{2h})\exp(-2jk_2 d \cos\theta_2)} \tag{26}$$

Using (26) to solve for $Z_{1h}$ produces

$$Z_{1h} =$$

$$\frac{Z_{2h}^2(1 - R_\perp)\left[1 - e^{-2jk_2 d \cos\theta_2}\right] - Z_{2h}Z_{3h}(1 + R_\perp)\left[1 + e^{-2jk_2 d \cos\theta_2}\right]}{Z_{3h}(1 + R_\perp)\left[1 - e^{-2jk_2 d \cos\theta_2}\right] - Z_{2h}(1 - R_\perp)\left[1 + e^{-2jk_2 d \cos\theta_2}\right]} = \frac{\omega\mu_o}{k_1\cos\theta_1} \tag{27}$$

Then, inverting (27) and squaring both sides results in

$$k_1^2 \cos^2\theta_1 = k_1^2 - k_o^2 \sin^2\theta_i =$$

$$\omega^2\mu_o^2 \left\{ \frac{Z_{3h}(1 + R_\perp)\left[1 - e^{-2jk_2 d \cos\theta_2}\right] - Z_{2h}(1 - R_\perp)\left[1 + e^{-2jk_2 d \cos\theta_2}\right]}{Z_{2h}^2(1 - R_\perp)\left[1 - e^{-2jk_2 d \cos\theta_2}\right] - Z_{2h}Z_{3h}(1 + R_\perp)\left[1 + e^{-2jk_2 d \cos\theta_2}\right]} \right\}^2 \tag{28}$$

Recognizing that $k_1^2$ can be written in terms of $\epsilon_1$ and $\sigma_1$ as $\omega^2\mu_0\epsilon_1 - j\omega\mu_0\sigma_1 = k_1^2$ and using this in (28) enables a final solution to be obtained for $\epsilon_1$ and $\sigma_1$:

$$\epsilon_{r1} = \sin^2\theta_i +$$

$$\frac{\mu_o}{\epsilon_o} \, \text{Re}\left\{ \frac{Z_{3h}(1 + R_\perp)\left[1 - e^{-2jk_2 d \cos\theta_2}\right] - Z_{2h}(1 - R_\perp)\left[1 + e^{-2jk_2 d \cos\theta_2}\right]}{Z_{2h}^2(1 - R_\perp)\left[1 - e^{-2jk_2 d \cos\theta_2}\right] - Z_{2h}Z_{3h}(1 + R_\perp)\left[1 + e^{-2jk_2 d \cos\theta_2}\right]} \right\}^2 \tag{29}$$

28

$$\sigma_1 = \omega\mu_o$$

$$\times \text{ Im} \left\{ \frac{Z_{3h}(1+R_\perp)\left[1-e^{-2jk_2 d\cos\theta_2}\right]-Z_{2h}(1-R_\perp)\left[1+e^{-2jk_2 d\cos\theta_2}\right]}{Z_{2h}^2(1-R_\perp)\left[1-e^{-2jk_2 d\cos\theta_2}\right]-Z_{2h}Z_{3h}(1+R_\perp)\left[1+e^{-2jk_2 d\cos\theta_2}\right]} \right\}^2$$

$$(30)$$

where

Re means take the real part of the expression and

Im means take the imaginary part of the expression.

The above two equations represent the final result of the derivation. The key to using (29) and (30) is in measuring $R_\perp$. Experimental work would have to focus on how well the amplitude and phase of the reflected field could be measured in determining $\epsilon_1$ and $\sigma_1$. Equations (29) and (30) were validated by choosing particular values for frequency, $\theta_i$, $\epsilon_2$, $\sigma_2$, $d$, $\epsilon_1$, and $\sigma_1$, which were then used to calculate $R_\perp$. This calculated value of $R_\perp$ was treated as having been obtained from measurements and was used in (29) and (30). The resulting values for $\epsilon_1$ and $\sigma_1$ were then compared to the original values used to compute $R_\perp$. It was found that equations (29) and (30) provide a valid means of solving for $\epsilon_1$ and $\sigma_1$.

**Calculating the Dielectric Constant and Conductivity for a Medium Beneath a Forest or Jungle Canopy —— Vertical Polarization.** Let's consider the forest canopy problem for the case where the incident wave is vertically polarized. The geometry of the problem remains as shown in figure 4. The total magnetic field in medium three ( $\underline{H}_3(\underline{r})$ ) can be written as follows:

$$\underline{H}_3(\underline{r}) = a_y H_o \left\{ e^{-jk_o z\cos\theta_i} + R_{\parallel}e^{jk_o z\cos\theta_i} \right\} e^{-jk_o x\sin\theta_i} \quad (31)$$

where

$H_o$ is the amplitude of the incident magnetic field

$R_{||}$ is the reflection coefficient

The reflection coefficient $R_{||}$ can be written in terms of the impedances of the three media involved:

$$R_{||} = \frac{Z_{3v} - Z_{inv}^{(2)}}{Z_{3v} + Z_{inv}^{(2)}} \qquad (32)$$

where

$$Z_{inv}^{(2)} = \frac{Z_{2v}(Z_{1v} + Z_{2v}) + Z_{2v}(Z_{1v} - Z_{2v})\exp(-2jk_2 d\cos\theta_2)}{Z_{1v} + Z_{2v} - (Z_{1v} - Z_{2v})\exp(-2jk_2 d\cos\theta_2)}$$

$$Z_{3v} = \frac{k_o \cos\theta_i}{\omega\epsilon_o} \qquad Z_{2v} = \frac{k_2 \cos\theta_2}{\omega(\epsilon_2 - j\sigma_2/\omega)} \qquad Z_{1v} = \frac{k_1 \cos\theta_1}{\omega(\epsilon_1 - j\sigma_1/\omega)}$$

$$k_o \sin\theta_i = k_1 \sin\theta_1 = k_2 \sin\theta_2 \qquad (33)$$

Once again, propagation constants for media 1 and 2 are complex. This will make the reflection coefficient complex so that it can be written as

$$R_{||} = \rho_{||} e^{j\phi_{||}} \qquad (34)$$

where $\rho_{||}$ is the magnitude of $R_{||}$ and $\phi_{||}$ is the phase. In figures 12 through 17, curves of $\rho_{||}$ versus angle of incidence are shown for the three materials discussed previously. The influence of the forest layer is not nearly so obvious in this case as it was for the horizontal polarization case where the oscillations in the curves clearly indicated the presence of a layer. The dip that occurs in the curves between the angles
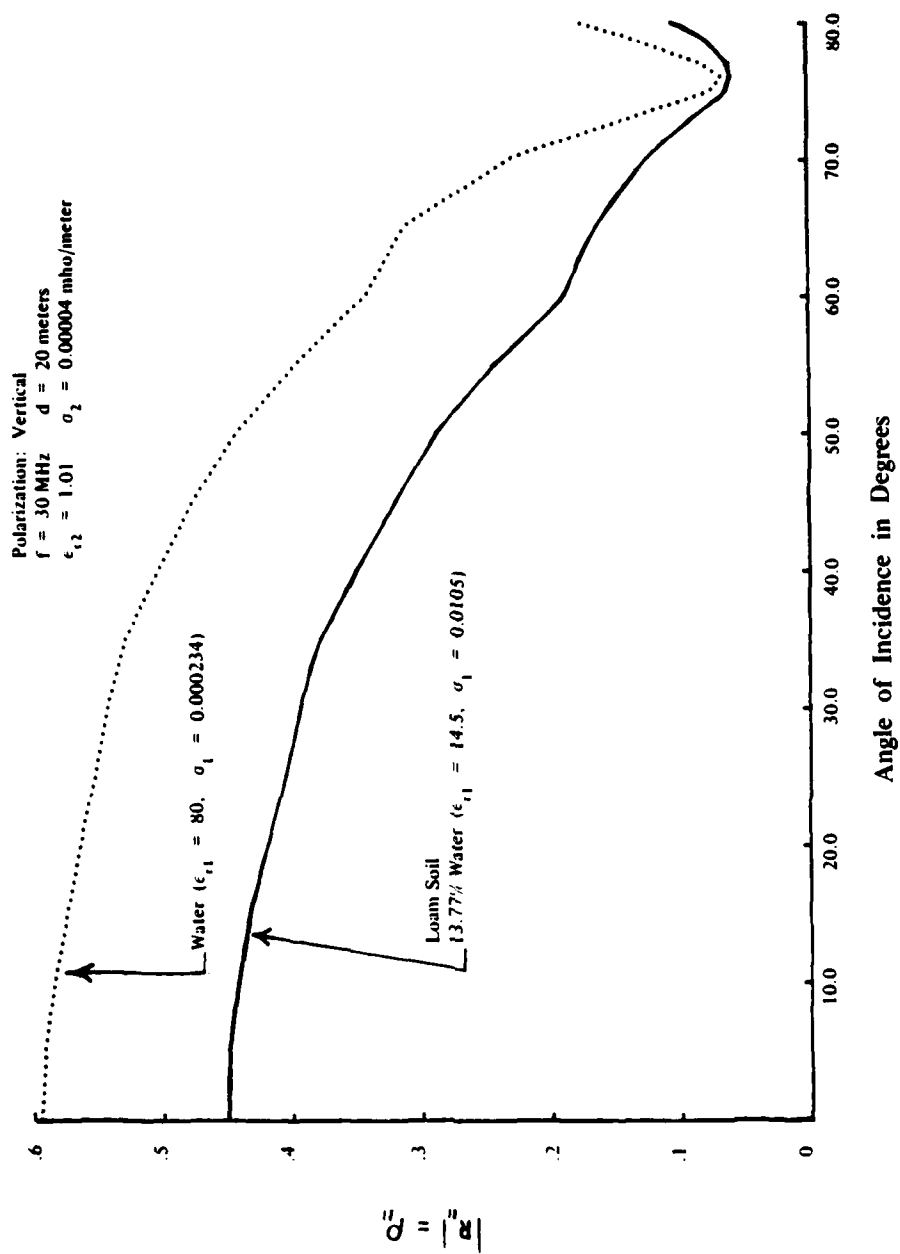
30

FIGURE 12. Study of Reflection Coefficient Versus Angle of Incidence – Vertical Polarization.
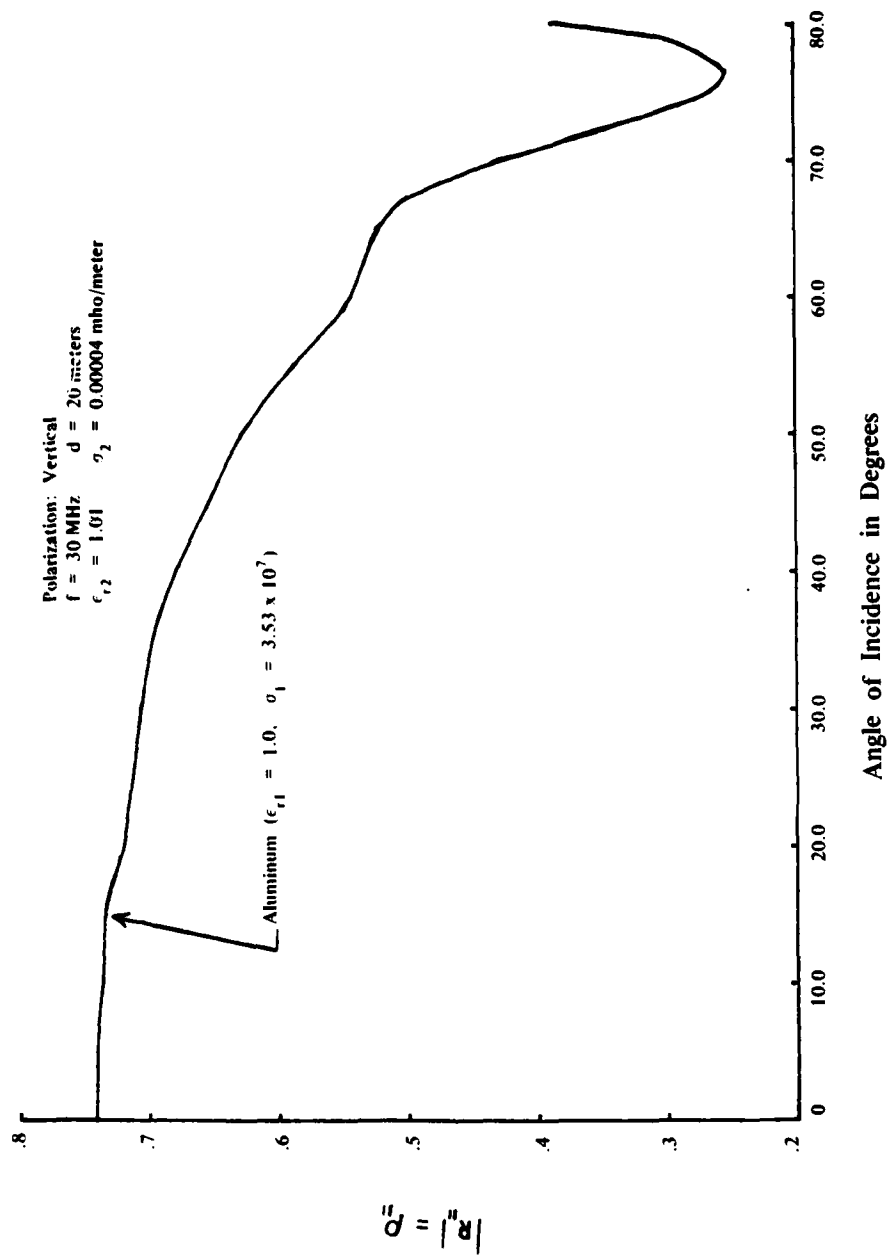
31

FIGURE 13. Study of Reflection Coefficient Versus Angle of Incidence -- Vertical Polarization.

32

FIGURE 14. Study of Reflection Coefficient Versus Angle of Incidence – Vertical Polarization.

33

Polarization: Vertical
$f$ = 20 MHz    $d$ = 20 meters
$\epsilon_{r2}$ = 1.01    $\sigma_2$ = 0.00004 mho/meter

Aluminum ($\epsilon_{r1}$ = 1.0,  $\sigma_1$ = 3.53 × 10^7)

$|R_{\parallel}| = \rho_{\parallel}$

Angle of Incidence in Degrees

FIGURE 15.  Study of Reflection Coefficient Versus Angle of Incidence — Vertical Polarization.

34

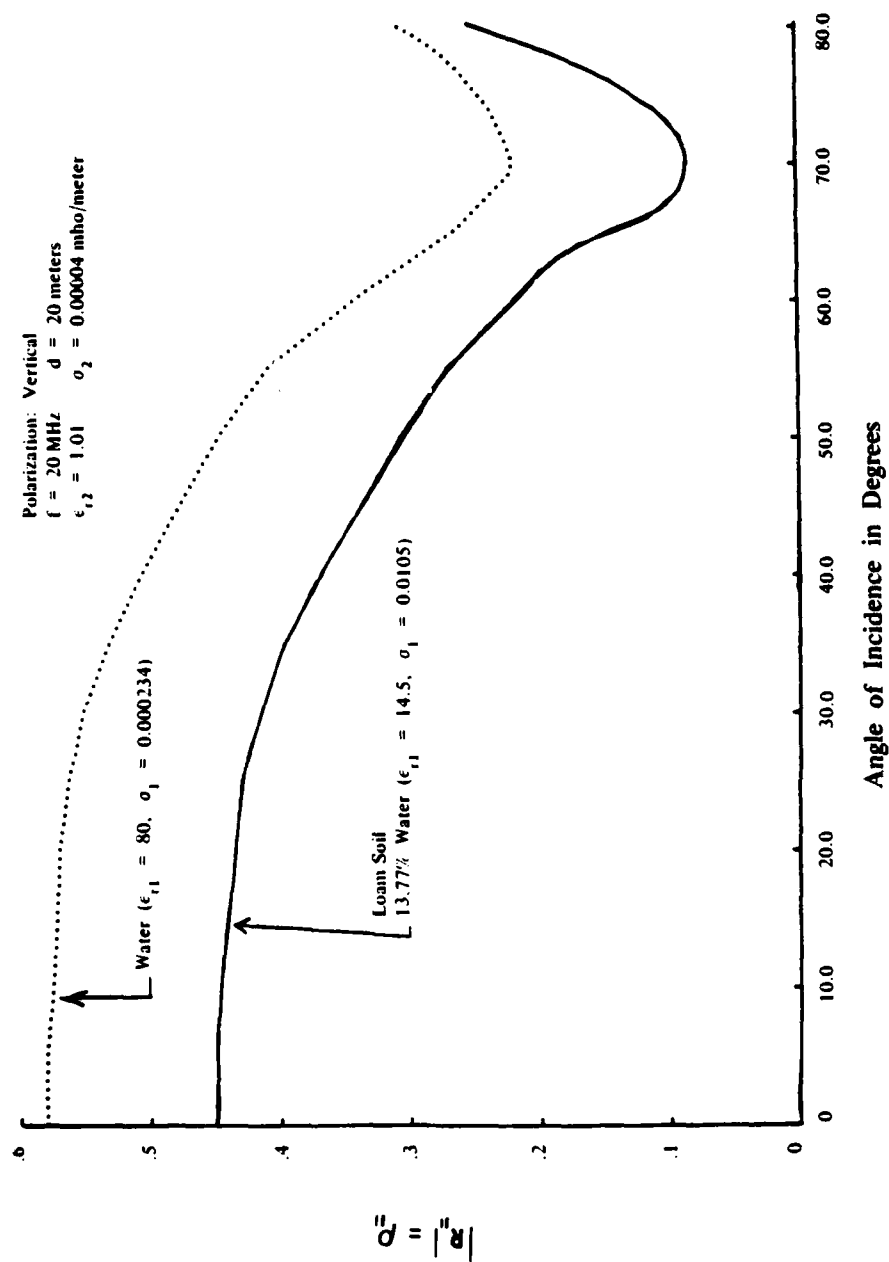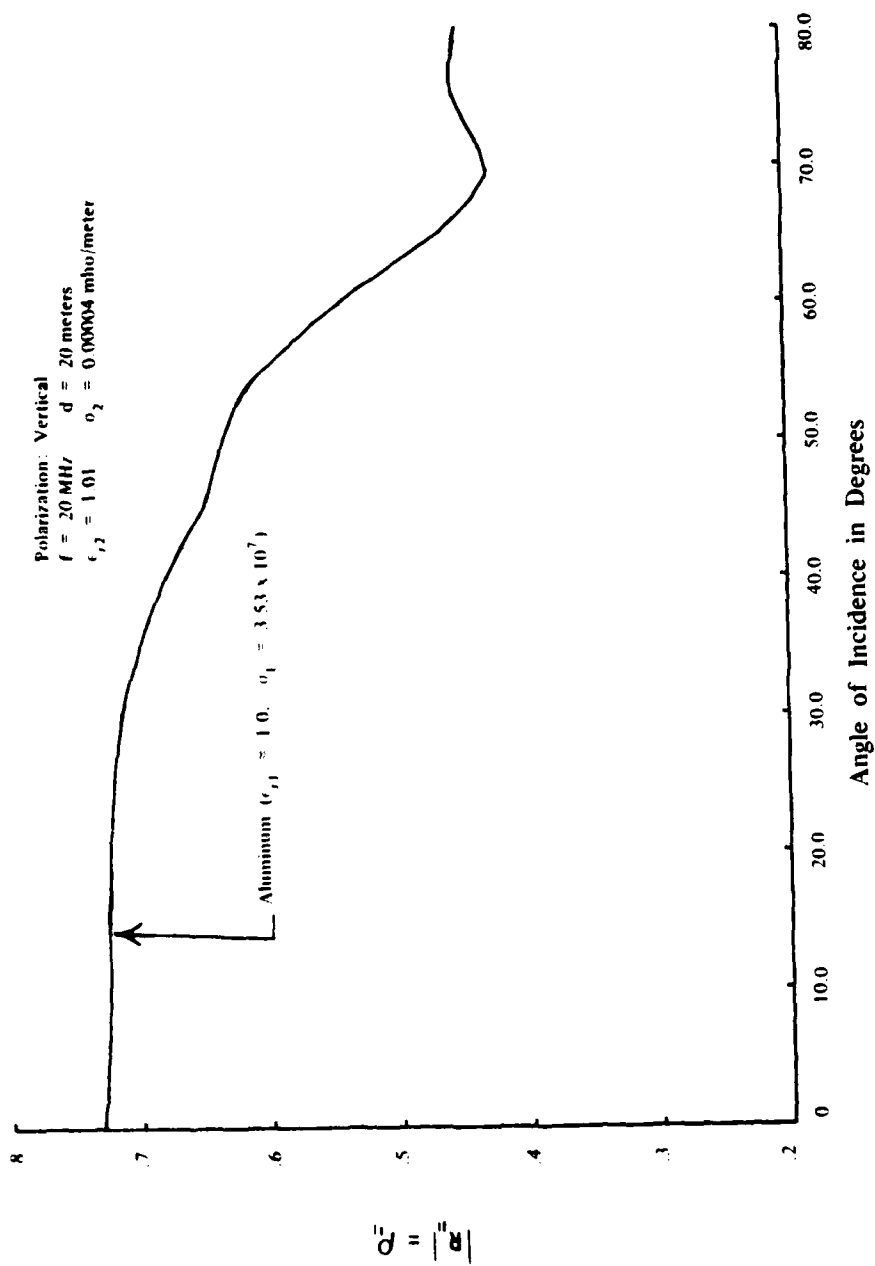FIGURE 16. Study of Reflection Coefficient Versus Angle of Incidence — Vertical Polarization.
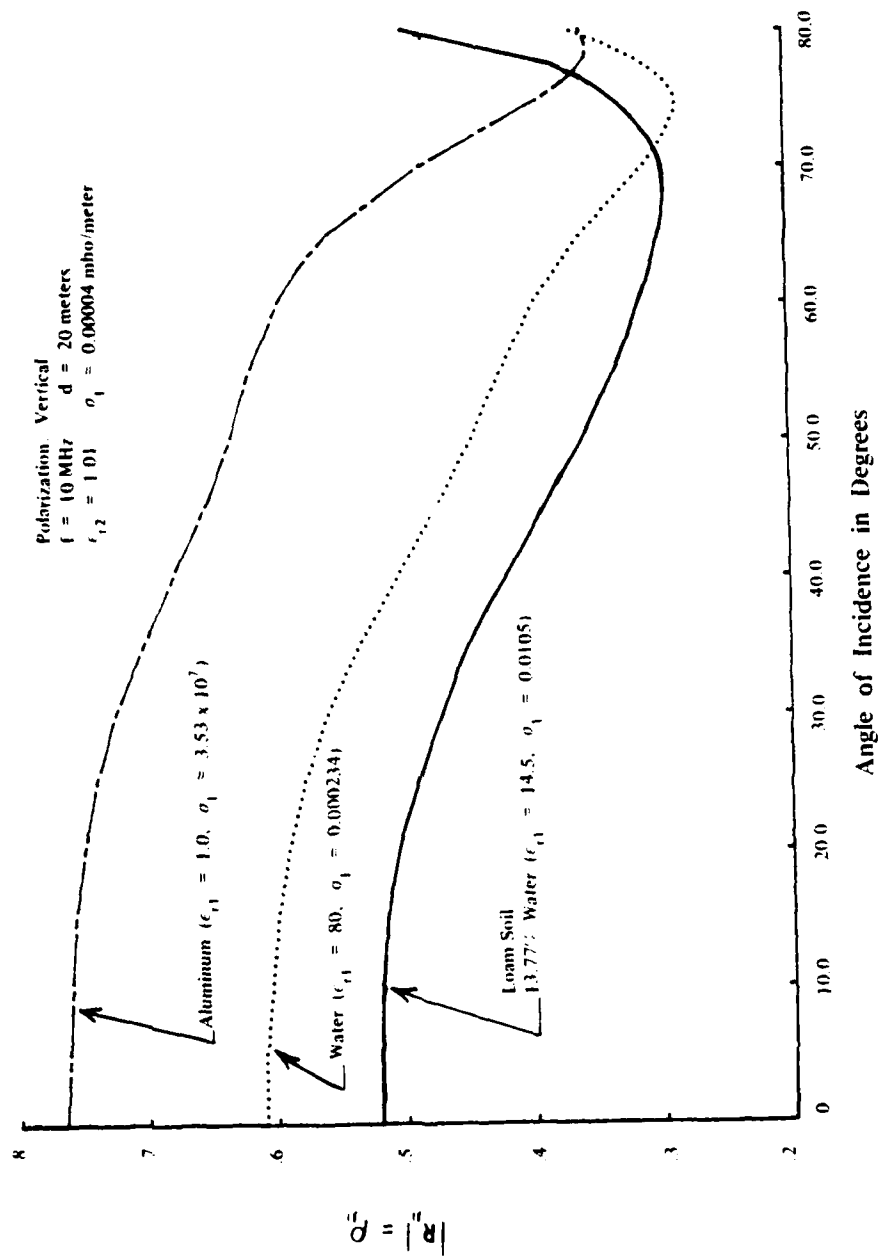
35

Polarization: Vertical
$f = 3$ MHz   $d = 20$ meters
$\epsilon_{r2} = 1.01$   $\sigma_2 = 0.00004$ mho/meter

Aluminum
$(\epsilon_{r1} = 1.0, \ \sigma_1 = 3.53 \times 10^7)$

Loam Soil
13.77/, Water ($\epsilon_{r1} = 14.5, \ \sigma_1 = 0.0105$)

Water ($\epsilon_{r1} = 80, \ \sigma_1 = 0.000234$)

$|R_{\shortparallel}| = \rho_{\shortparallel}$

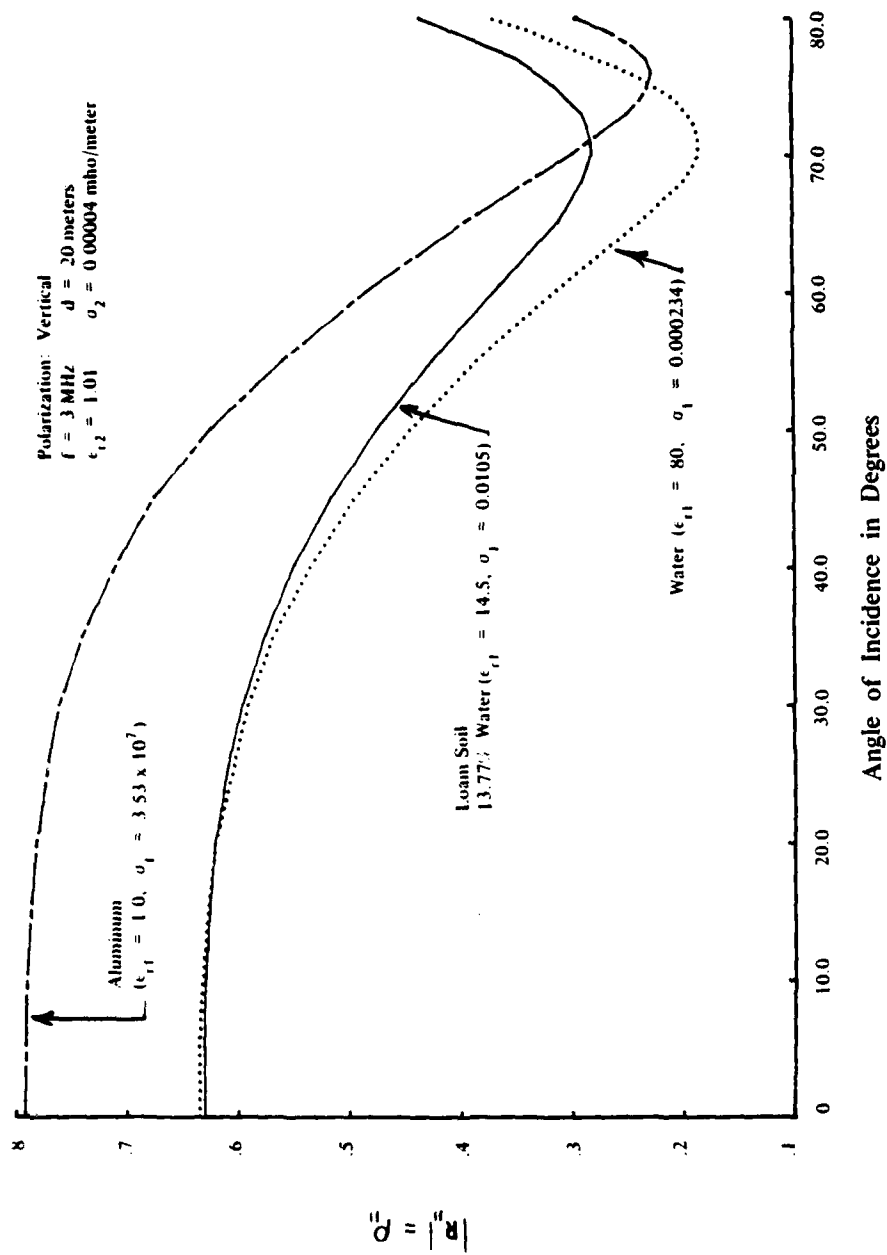Angle of Incidence in Degrees

FIGURE 17. Study of Reflection Coefficient Versus Angle of Incidence — Vertical Polarization.

36

of $70°$ and $80°$ is a Brewster angle effect. In figures 18 and 19, curves of phase versus angle of incidence are shown for loam soil and water. In figure 20, curves of $\rho_{||}$ versus frequency are shown for the three different materials and at an angle of incidence of 30 degrees. As in the horizontal polarization cases, assume that the magnitude and the phase of the reflection cofficient are measured and are available to determine the electrical properties $\epsilon_1$ and $\sigma_1$. Using equations (32) and (33), one obtains an expression for $Z_{1v}$:

$$Z_{1v} =$$

$$\frac{Z_{2v}\left[Z_{3v}(1-R_{||})(1+e^{-2jk_2 d \cos \theta_2}) - Z_{2v}(1+R_{||})(1-e^{-2jk_2 d \cos \theta_2})\right]}{Z_{2v}(1+R_{||})(1+e^{-2jk_2 d \cos \theta_2}) - Z_{3v}(1-R_{||})(1-e^{-2jk_2 d \cos \theta_2})} \tag{35}$$

Letting the quantity on the right side of (35) be equal to g and using the definition of $Z_{1v}$ results in

$$\frac{k_1 \cos \theta_1}{\omega \epsilon_1 - j\sigma_1} = g \tag{36}$$

Multiplying the numerator and denominator on the left hand side of (36) by $\omega\mu_0$ and realizing that $k_1^2 = -j\omega\mu_0\sigma_1 + \omega^2\mu_0\epsilon_1$ one obtains

$$g = \frac{\omega\mu_0 \cos \theta_1}{k_1} \tag{37}$$

Squaring (37), multiplying the numerator and denominator on the right side of (37) by $k_1^2$, and substituting $1 - \sin^2 \theta_1$ for $\cos^2 \theta_1$ results in

$$\frac{\omega^2\mu_0^2 k_1^2 (1 - \sin^2 \theta_1)}{k_1^2} = k_1^2 g^2 \tag{38}$$
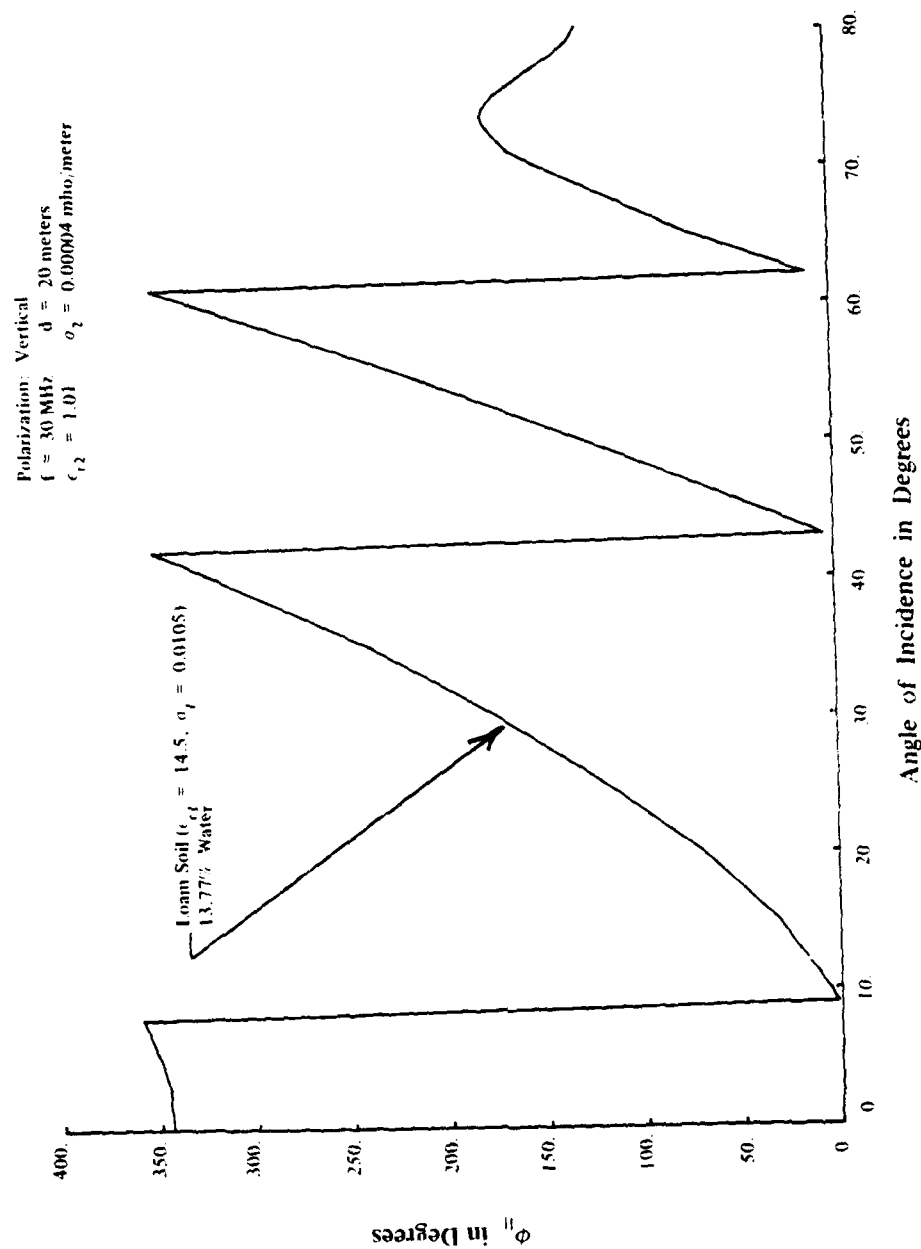
37

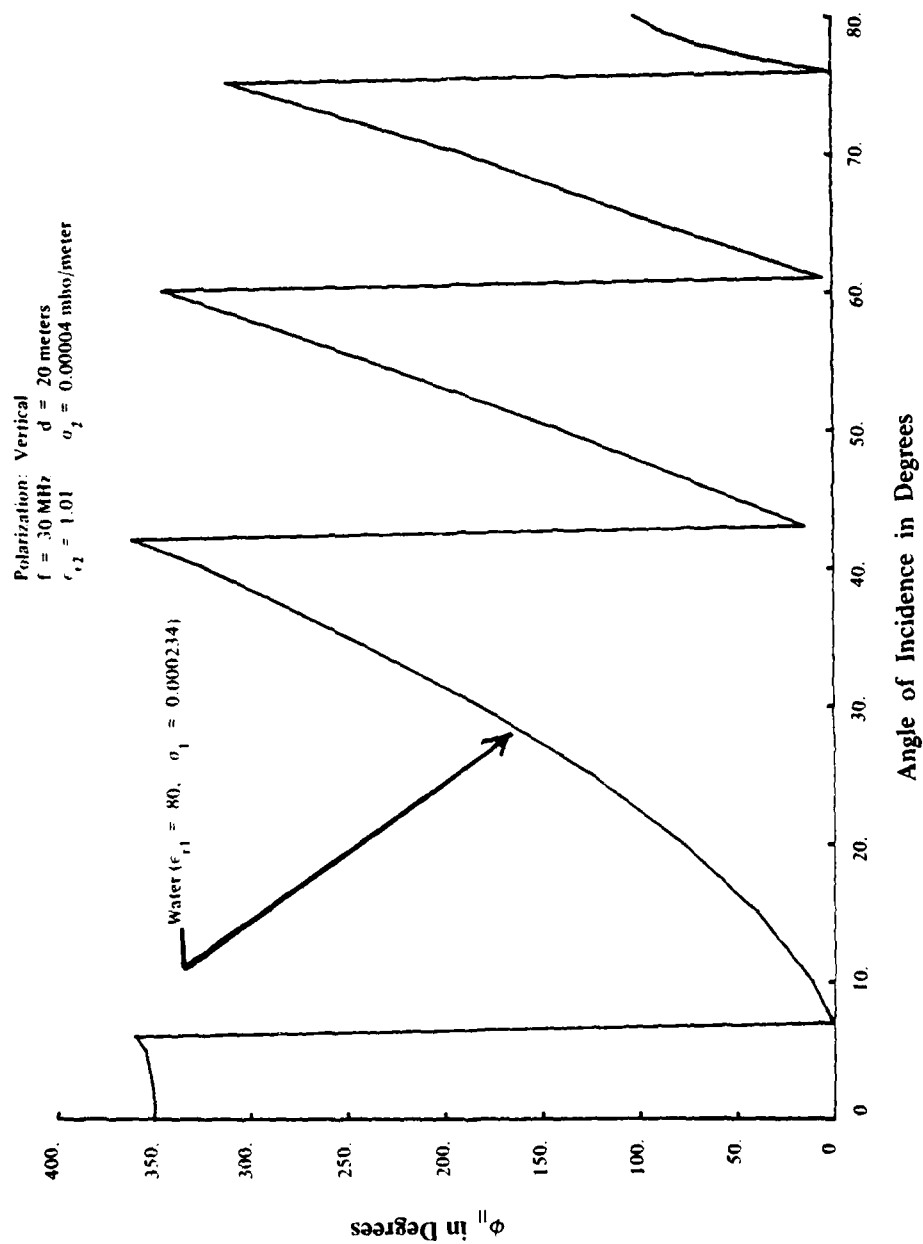FIGURE 18. Study of Phase Versus Angle of Incidence for Loam Soil – Vertical Polarization.

38

FIGURE 19. Study of Phase Versus Angle of Incidence for Water – Vertical Polarization.
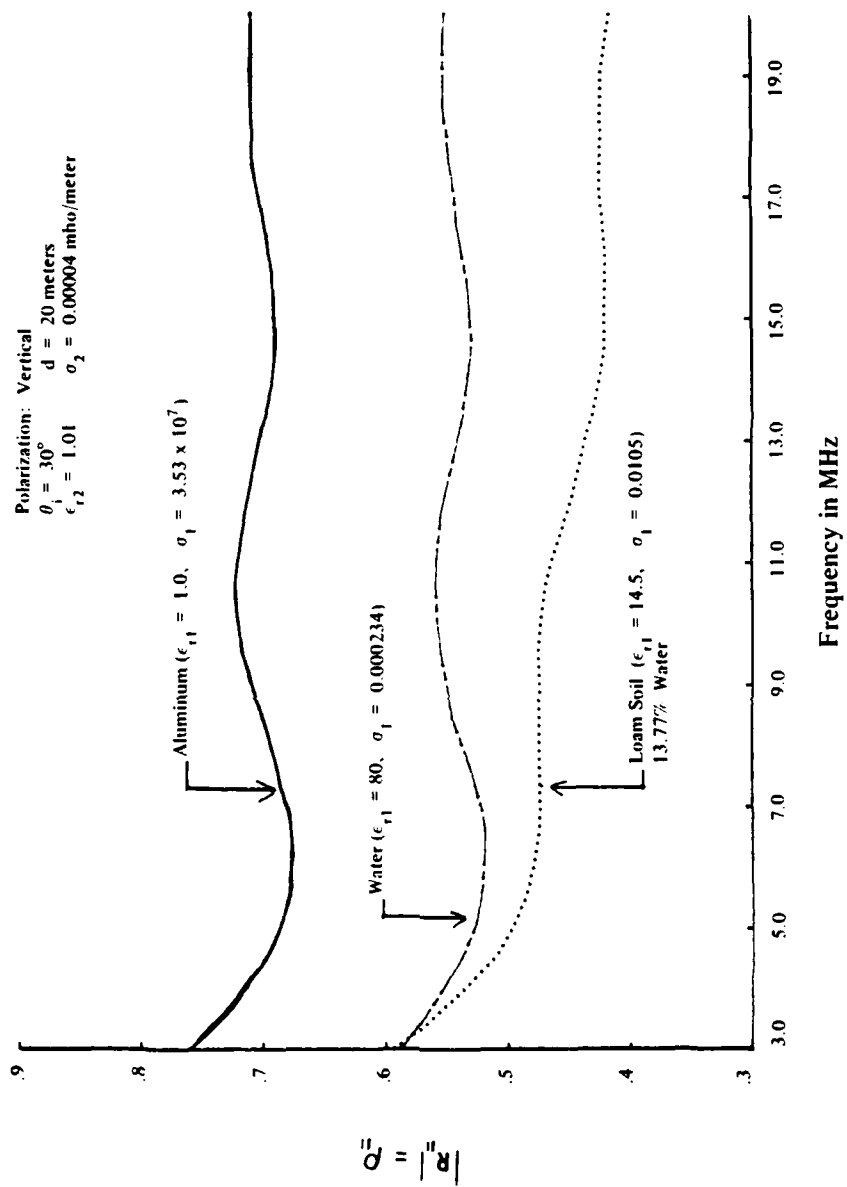
FIGURE 20. Study of Reflection Coefficient Versus Frequency – Vertical Polarization.

40

Recognizing that $k_1 \sin \theta_1 = k_o \sin \theta_i$, one can write equation (38) as follows:

$$k_1^4 g^2 - \omega^2 \mu_o^2 k_1^2 + \omega^2 \mu_o^2 k_o^2 \sin^2 \theta_i = 0 \tag{39}$$

Equation (39) is a fourth degree equation for $k_1$, which can be solved by letting $k_1^2 = \xi$:

$$\xi^2 g^2 - \omega^2 \mu_o^2 \xi + \omega^2 \mu_o^2 k_o^2 \sin^2 \theta_i = 0 \tag{40}$$

A solution for $\xi$ can now be obtained:

$$\xi = \frac{\omega^2 \mu_o^2 \pm \sqrt{\omega^4 \mu_o^4 - 4g^2 \omega^2 \mu_o^2 k_o^2 \sin^2 \theta_i}}{2g^2} \tag{41}$$

The problem of which sign to use in (41) is easily resolved by seeing what happens at $\theta_i = 0°$. When $\theta_i = 0°$ in (41) and the minus sign is used, the totally unrealizable result of $\xi = 0$ is obtained. This indicates clearly that the proper sign to choose in (41) is the plus sign. Because $\xi = k_1^2$ we now have

$$k_1^2 = -j\omega\mu_o\sigma_1 + \omega^2\mu_o\epsilon_1 = \omega^2\mu_o^2 \left[ \frac{1 + \sqrt{1 - 4g^2 \epsilon_o \sin^2 \theta_i / \mu_o}}{2g^2} \right] \tag{42}$$

In the above equation. $k_o = \omega\sqrt{\mu_o \epsilon_o}$. It is now possible to solve for $\epsilon_1$ and $\sigma_1$.

$$\epsilon_1 = \epsilon_{r1}\epsilon_o = \mu_o \, \mathrm{Re} \left\{ \frac{1 + \sqrt{1 - 4g^2 \epsilon_o \sin^2 \theta_i / \mu_o}}{2g^2} \right\} \tag{43}$$

41

$$\sigma_1 = -\omega\mu_o \ \text{Im} \ \left\{ \frac{1 + \sqrt{1 - 4g^2 \, \epsilon_o \sin^2 \theta_i / \mu_o}}{2g^2} \right\} \tag{44}$$

Equations (43) and (44) are the final desired results. One can see how formidable the results are if the right hand side of (35) is substituted for g. The above equations were validated using the same method that was used for horizontal polarization. Particular values were chosen for frequency, $\theta_i$, $\epsilon_2$, $\sigma_2$, d, $\epsilon_1$, and $\sigma_1$; Then, these were used to compute $R_{||}$. The computed value of $R_{||}$ was then considered as a measured quantity and used in (43) and (44) to compute $\epsilon_1$ and $\sigma_1$. These resulting values for $\epsilon_1$ and $\sigma_1$ were compared to the original values of $\epsilon_1$ and $\sigma_1$ that were used to compute $R_{||}$. By following this method, it was shown that (43) and (44) are a valid way of computing $\epsilon_1$ and $\sigma_1$.

In the following section, the results that were obtained will be discussed along with using radar imagery to extract terrain feature information.

## DISCUSSION

In the previous section, several examples of inverse problems were considered. First, inverse scattering was examined for discrete objects. However, this particular problem has very little application toward determining terrain feature parameters because terrain consists of collections of scatterers that are placed more or less randomly in space. The physics of the problem of scattering from the collection of objects is different than that for a single object by itself. Also, the infinite conductivity assumption is not valid for any natural terrain feature.

Next, profile inversion was examined. This type of inverse problem also appears to have little application in determining terrain feature parameters, unless one is interested in computing the dielectric or conductivity profile in the earth's surface.

In addition, the problem of calculating the dielectric constant of a slightly rough surface using radar backscatter data from two polarizations was considered. The solution for this problem might be useful in determining the moisture content in a soil. An experimental measurements program would have to be set up to see how well the dielectric constant and moisture content could be determined from actual data. Also, the measurements program would have to include the collection of ground truth data in the way of dielectric constants, moisture contents, and perhaps surface roughness properties. The initial experimental work could be performed using a radar system such as the one at the University of Kansas.

The final problem considered was the calculation of the electrical properties beneath a forest or jungle canopy. A solution for this problem is important when one is trying to ascertain the nature of terrain materials located under a forest canopy. The electrical properties of the ground were computed in terms of a measured reflection coefficient, the height of the forest, and the electrical properties of the forest. Once again, a measurements program would have to be conducted in order to test the technique. One type of inverse problem that has not been considered as yet is that of using side-looking airborne radar imagery to infer various terrain features. This problem will be considered in the following paragraphs.

The average gray shade on a radar image over an area the size of a resolution cell is related to the value of the radar backscatter coefficient ( $\sigma^\circ$ ). This backscatter coefficient is a function of both system and terrain parameters as indicated below:

$$\sigma^\circ = f(\lambda, \theta_i, P_i, P_r, \Gamma_s, V_s, S_u, \hat{\epsilon}, Z_x, Z_y)$$

Theoretical expressions for $\sigma^\circ$ have been derived for certain types of rough surfaces, vegetation, and snow. The theoretical efforts, however, are just beginning to explain certain aspects of measured data, and much effort is needed in this area yet. In the above expression for $\sigma^\circ$, the following notation has been used:

### Radar System Parameters

$\lambda$ = radar wavelength

$\theta_i$ = local angle of incidence

$P_i$ = polarization of the incident wave

$P_r$ = polarization of the received wave

### Terrain Parameters

$\Gamma_s$ = surface roughness properties

$V_s$ = volume scattering affects such as those occurring in vegetation and snow.

$S_u$ = subsurface scattering affects

$\hat{\epsilon}$ = complex dielectric constant of the terrain surface

$Z_x$ and $Z_y$ = two orthogonal slopes of the terrain surface

Variations in gray shade from one resolution cell to another are due to changes in $\sigma°$, which in turn is due to changes in one or more of the above parameters. Interpretating radar imagery consists of trying to infer terrain features from the tonal variations on the image. The radar image interpreter should have a good understanding of how each of the system and terrain parameters influences $\sigma°$. This understanding can be obtained by analyzing and developing theoretical models and by analyzing experimental data. A great deal of research effort has gone into radar image interpretation using human photointerpreters. Also, people who were trained as interpreters of aerial photography have been used to analyze radar imagery. However, these photointerpreters do not have the necessary theoretical background to enable them to pinpoint specific parameter influences, which has tended to keep radar image interpretation largely in a heuristic state. One area of radar image analysis that has not received much attention is that of applying digital image processing methods. Analyzing radar imagery with various texture measures appears to be worthy research, if appropriate ground truth information can be obtained.

44

# CONCLUSIONS

As a result of this study, the following conclusions can be made:

1. Inverse scattering solutions for discrete objects are not applicable in determining terrain features.

2. Profile inversion solutions appear to have only a slight applicability in determining terrain features.

3. The problem of determining the dielectric constant of a slightly rough surface can be solved using the horizontal and vertically polarized backscatter coefficients, along with a Newton-Raphson numerical methods technique.

4. A solution for the dielectric constant and the conductivity of a medium located beneath a forest canopy can be obtained in terms of the amplitude and phase of the reflected wave.

DATE
FILMED

0-8